Nonlinear Dyn (2022) 110:963–994
https://doi.org/10.1007/s11071-022-07700-3

REVIEW

A review on the nonlinear dynamics of hyperelastic structures

Hossein B. Khaniki · Mergen H. Ghayesh · Rey Chin · Marco Amabili

Received: 19 March 2022 / Accepted: 11 July 2022 / Published online: 5 August 2022

Abstract This paper presents a critical review of the nonlinear dynamics of hyperelastic structures. Hyperelastic structures often undergo large strains when subjected to external time-dependent forces. Hyperelasticity requires specific constitutive laws to describe the mechanical properties of different materials, which are characterised by a nonlinear relationship between stress and strain. Due to recent recognition of the high potential of hyperelastic structures in soft robots and other applications, and the capability of hyperelasticity to model soft biological tissues, the number of studies on hyperelastic structures and materials has grown significantly. Thus, a comprehensive explanation of hyperelastic constitutive laws is presented, and different techniques of continuum mechanics, which are suitable to model these materials, are discussed in this literature review. Furthermore, the sensitivity of each hyperelastic strain energy density function to coefficient variation is shown for some well-known hyperelastic models. Alongside this, the application of hyperelasticity to model the nonlinear dynamics of polymeric structures (e.g., beams, plates, shells, membranes and balloons) is discussed in detail with the assistance of previous studies in this field. The advantages and disadvantages of hyperelastic models are discussed in detail. This present review can stimulate the development of more accurate and reliable models.

Keywords Nonlinear dynamics · Hyperelasticity · Hyperelastic beams · Hyperelastic plates · Hyperelastic shells · Nonlinear elasticity

H. B. Khaniki (✉) · M. H. Ghayesh (✉) · R. Chin
School of Mechanical Engineering, University of Adelaide, Adelaide, South Australia 5005, Australia
e-mail: hossein.bakhshikhaniki@adelaide.edu.au

M. H. Ghayesh
e-mail: mergen.ghayesh@adelaide.edu.au

R. Chin
e-mail: rey.chin@adelaide.edu.au

M. Amabili
Department of Mechanical Engineering, McGill University, 817 Sherbrooke Street West, Montreal H3A 0C3, Canada
e-mail: marco.amabili@mcgill.ca

1 Introduction

Hyperelastic structures often undergo large strains when subjected to external forces. The stress–strain relation in such structures is highly complicated, making the linear stress–strain relationship and linear elastic models invalid for simulating their mechanical behaviour. The hyperelastic behaviour can be seen in different soft structures such as rubbers, foams and human body organs. Along with understanding the characteristics of such structures, having accurate modelling of hyperelastic structures could also

provide us with further potential applications in different fields.

1.1 Necessity for this review

By analysing the available database in Scopus on *hyperelasticity*, the significance of the dialogue between scientists and researchers on this topic was obtained. Figure 1a demonstrates the number of published works on *hyperelasticity* from 1990 to 2020. It can be seen that, during this period, the number of published papers on this subject has increased noticeably, reaching more than 1100 research studies published in 2020 alone.

Moreover, analysing the mechanical behaviours (bending, buckling and vibration) of hyperelastic structures (e.g. beams, plates, shells and membranes) shows the same incremental trend indicated in Fig. 1b; from which it can be seen that many studies on hyperelasticity are focused on the mechanics of such structures. The phenomenal growth of studies on this subject clarifies the importance of having a systematic literature review to summarise the achievements to date on this topic.

1.2 Applications of hyperelastic structures

In general, soft structures present hyperelastic behaviours while confronting different conditions. One of the main applications of hyperelastic structures is soft robotics [1–3]; since soft structures can provide higher-order degrees of freedom, movement in robotic

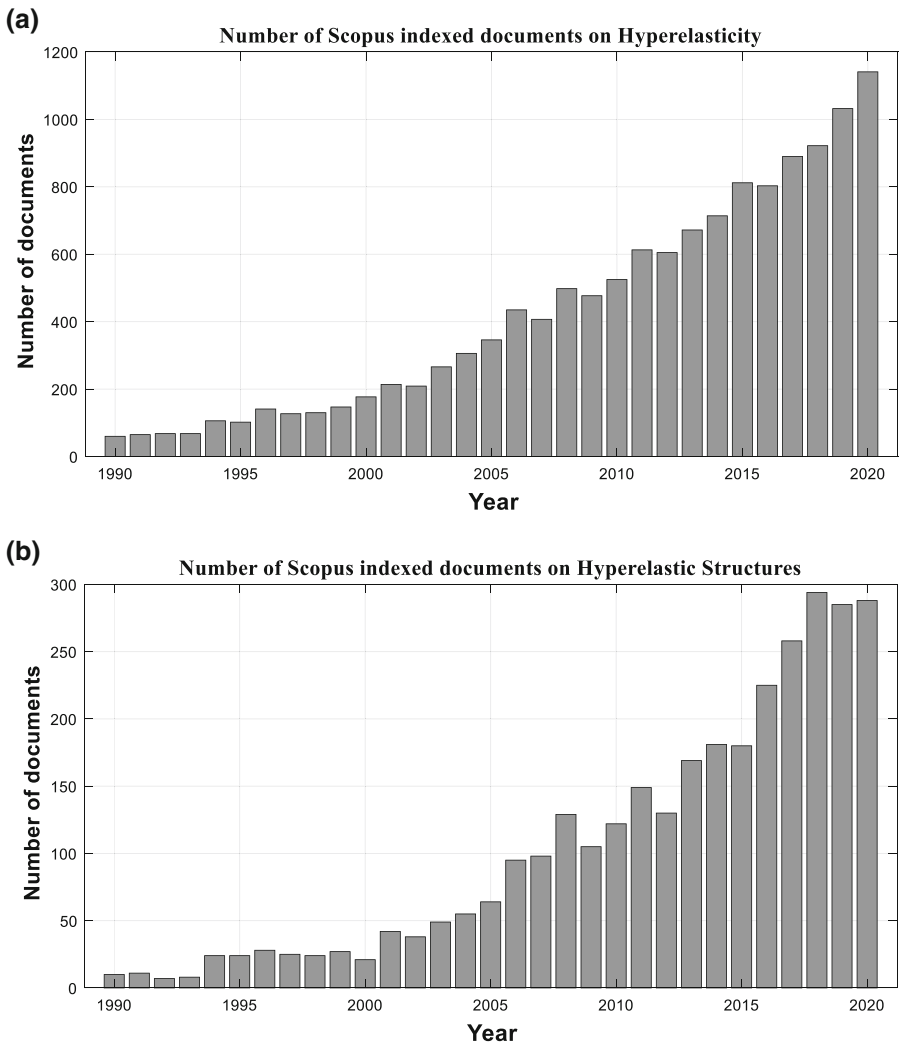

Fig. 1 Tables for the number of documents from 1990 to 2020 on (**a**) hyperelasticity and (**b**) hyperelastic beams, plates and shells

parts could potentially become more smooth than when using rigid and/or firm structures.

Robotic rehabilitation systems for stroke patients can be significantly improved by using soft robotic as they can provide a smooth motion with a safer operation [4]. For instance, soft robotic gloves are capable of helping patients with muscular dystrophy, amyotrophic lateral sclerosis or post-stroke hand function assistance [5–8]. In the work presented by Polygerinos et al. [4], a soft robotic glove is presented to study the hand and fingers' joint motion. In their model, the different mechanical behaviours of bending, twisting and extensions of soft beam-shaped structures were obtained.

Developing soft structures to explore unknown environments is another important application of hyperelastic structures as it can tolerate different types of loadings and impacts. In a study done by Antol et al. [9], it is shown that expensive wheel rovers can be replaced with tumbleweed rovers for Mars exploration. In another study, Trivedi et al. [10] used hyperelastic tubes for soft robotic modelling of Oct-Arm.

Besides, soft robots made of hyperelastic materials have been used for sensing and monitoring environments. For example, a dragonfly-inspired soft robot (DraBot) has been fabricated for measuring the contaminants (such as the presence of oil), pH, and temperature of water surfaces [11–13].

The application of hyperelastic structures in soft robotics has reached a turning point with the capability of 3D printing and the utilisation of soft actuators [14–16]. Hyperelastic structures also have other types of applications, of which some of the main ones are wearable devices [17], stretchable electronics [17], biomedical engineering [17], and energy harvesters [18, 19].

Figure 2 presents a simple robot that is capable of crawling using twisted and coiled actuators [20]. This simple model has been fabricated using hyperelastic beams, and the smooth motion of the robot was obtained by bending. Figure 3 also presents some useful examples of soft structures as actuators in soft robotics, which can be used for grabbing, twisting, motion, lifting and other purposes [15].

Another application of soft structures can be found in belt operating systems. Belt conveyor systems are mainly used for power transmission from the driving

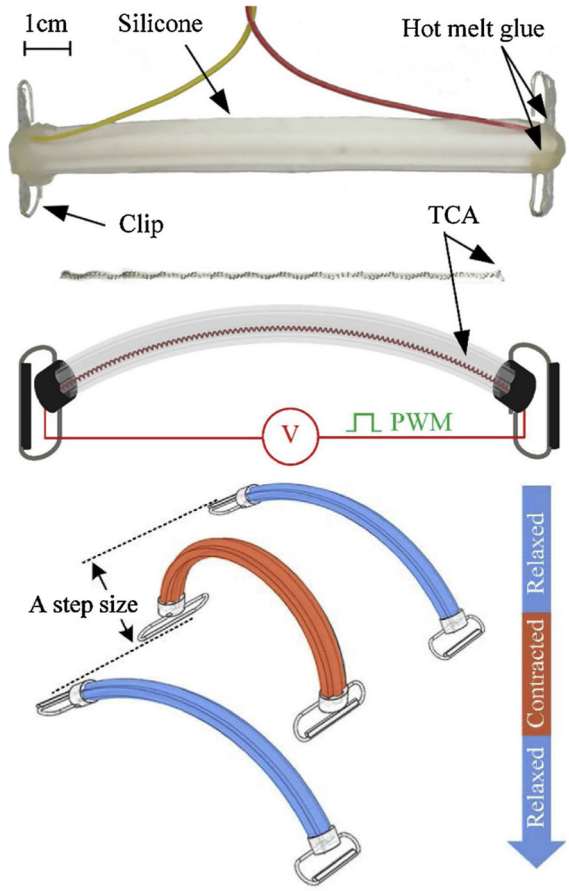

Fig. 2 Schematic view of a crawling robot using soft structures [20]. (Permission obtained from Elsevier)

pulley to the driver one in different engineering fields [21–23].

Layered hyperelastic structures have been used for packaging, especially food industry, as a soft safe layer is required for inside and a stiffer layer for outside. The proper design and material usage are of high importance as the packaging is around 15% of the total variable costs [24, 25]. Waste management and environmentally friendly (biodegradable) packaging [26–28] are also important topics making the discussion of using proper hyperelastic materials for packaging an ongoing novel research topic.

Since human body organs show nonlinear elastic behaviour, researchers have worked on fabricating prosthetics with similar hyperelastic behaviour. Using hyperelastic structures for firstly modelling the human body organs and secondly accurately designing

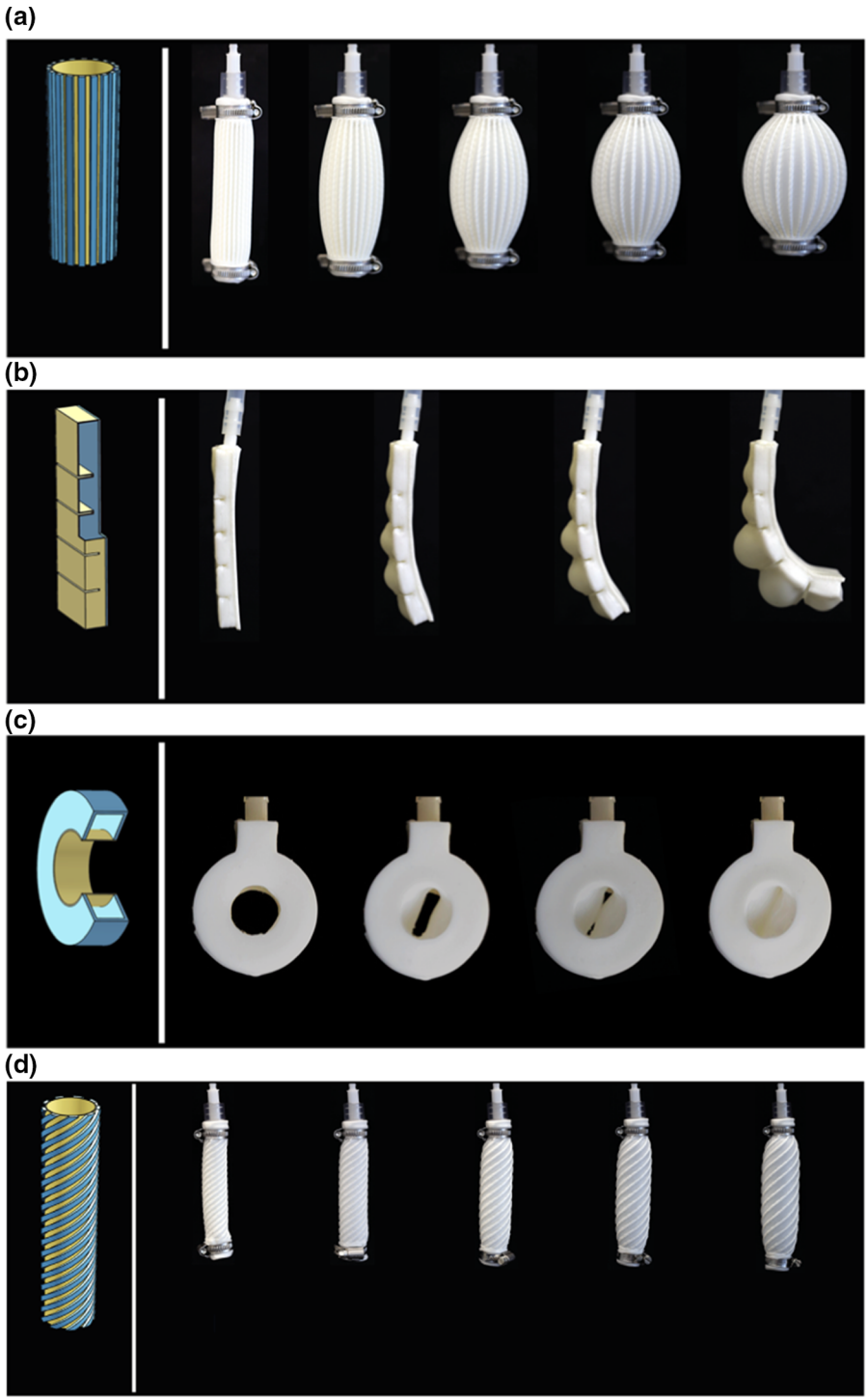

Fig. 3 Actuators made of soft structures with different purposes: **a** contractor; **b** bender; **c** grabber; **d** twister [15]. (This article is an open access article distributed under the terms and conditions of the Creative Commons Attribution (CC BY) license (https://creativecommons.org/licenses/by/4.0/).)

prosthetics have been a novel topic for researchers to invest [29–32].

1.3 Contribution of this paper to the field

The importance of modelling hyperelastic structures accurately has been discussed in the previous subsections. It is shown that there has been a considerable number of researches on hyperelasticity with promising, growing trends over the past few years. The demonstration of the high application potential of these structures in the early years of their development and their future in engineering design [14, 15, 20, 33, 34] emphasises the necessity of having a systematic literature review through the need for categorisation, discussion and explanation of the achievements to date. Accordingly, this review intends to clarify the achievements and goals of this research field by analysing diverse critical hyperelastic studies in the framework of nonlinear dynamics.

1.4 Structure of this review paper

To present a comprehensive investigation on hyperelastic structures, this review is structured in the following order: as shown in the flowchart of Fig. 4, in Sect. 1, a brief introduction to hyperelastic structures is given, indicating the importance of understanding the hyperelastic mechanical behaviour, emphasizing the application's potential and the future of hyperelastic structures, and lastly, demonstrating the contribution of this review to this field. In Sect. 2, some well-known constitutive hyperelastic models for isotropic soft materials are discussed in detail by presenting the fundamental continuum mechanics formulation and definitions related to hyperelastic behaviour. Some of the well-known techniques and models in continuum mechanics are then provided, followed by the sensitivity of the model in tracking hyperelastic behaviour. In Sect. 3, the application of the given and other hyperelastic continuum models on obtaining the nonlinear dynamics of hyperelastic beam structures is discussed. Section 4 concentrates on analysing hyperelastic plate and shell structures in

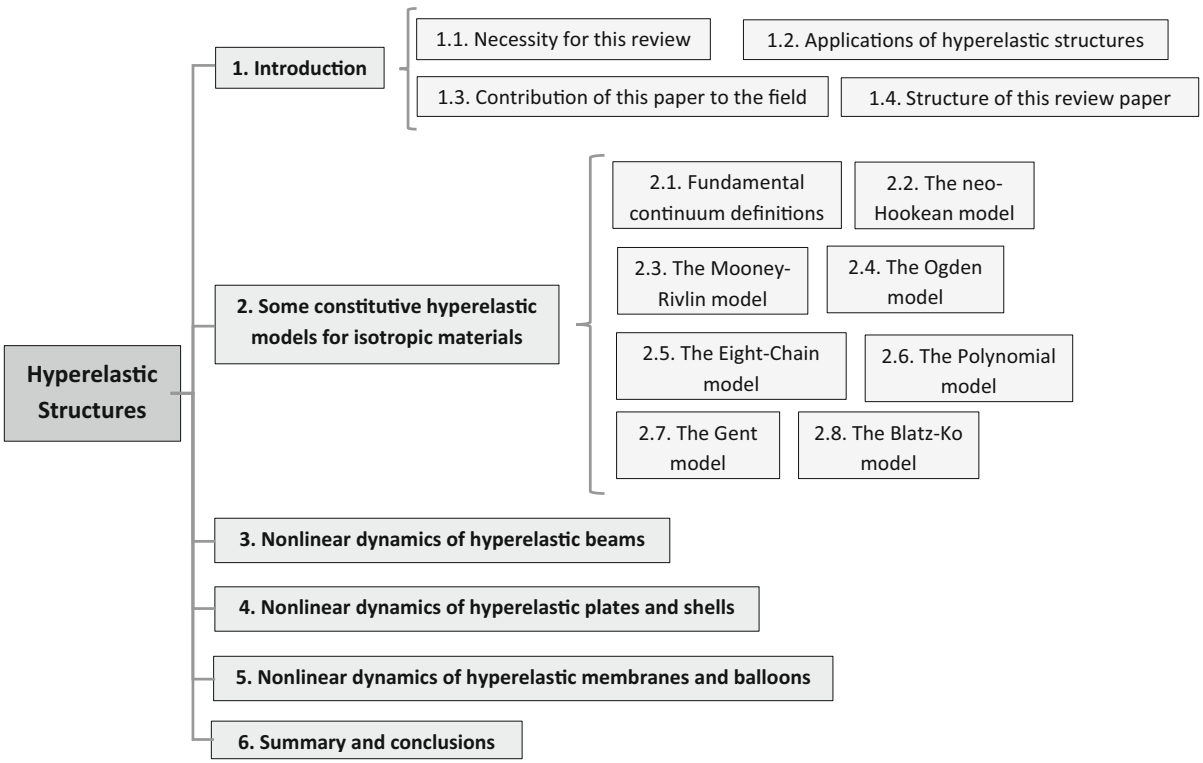

Fig. 4 Flowchart of the structure of this review

the framework of nonlinear dynamics. Different plate and shell theories together with hyperelastic constitutive models are discussed for accurately modelling the nonlinear dynamics of soft plate and shell structures. Section 5 presents a detailed explanation on hyperelastic models and nonlinear dynamics of soft membranes and balloons using different continuum mechanics models. Lastly, in Sect. 6, a comprehensive summary of the analysis performed through this paper is provided, and the achievements and possible potential for improving the modelling of such structures are presented.

2 Some constitutive hyperelastic models for isotropic materials

2.1 Fundamental continuum definitions

In order to define the mechanical characteristics of hyperelastic structures, there are key continuum mechanics definitions that must be presented. In general, the deformation gradient (F) is defined as [35]:

$$\begin{cases} F_{ij} = \delta_{ij} + \dfrac{\partial u_i}{\partial x_j}, \\ J = \det(F), \end{cases} \tag{1}$$

with J is the determinant of the deformation gradient, δ is the Kronecker delta and u_i is the displacement field, which could be rewritten in the principal directions of the structures as [36]:

$$F = \begin{bmatrix} \lambda_1 & 0 & 0 \\ 0 & \lambda_2 & 0 \\ 0 & 0 & \lambda_3 \end{bmatrix} \quad \rightarrow \quad F_{ij} = \delta_{ij}\lambda_i, \tag{2}$$

where λ_i indicates the principal stretch through the principal direction i, defined as

$$\lambda_i = \frac{L_i}{L_i^0}, \tag{3}$$

with L_i and $L_i.^0$ are the deformed and undeformed lengths of the structure through the i direction, respectively. Another important definition in describing hyperelastic structures is the left Cauchy–Green strain tensor (B) which is [36]

$$B = F \cdot F^T \quad \rightarrow \quad B_{ij} = F_{ik}F_{jk} \tag{4}$$

For conventional definitions, the left Cauchy–Green strain tensor's invariants are defined as [37]:

$$\begin{aligned} I_1 &= \frac{Tr(B)}{J^{\frac{2}{3}}} = \frac{B_{ii}}{J^{\frac{2}{3}}}, \\ I_2 &= \frac{1}{2}\left(I_1^2 - \frac{B_{ij}B_{ji}}{J^{\frac{4}{3}}}\right), \\ I_3 &= J^2, \end{aligned} \tag{5}$$

where I_1, I_2 and I_3 are the first, second and third strain invariants for compressible structures, respectively; for incompressible analysis, the first and second invariants will be simplified by having $J = 1$ and the third invariant will be equal to 1 (interested readers are referred to Refs. [38–40] for more information regarding compressible and incompressible materials). The Green–Lagrange strain–displacement can be written regarding the deformation gradient as:

$$E = \frac{1}{2}\left(F^T F - I\right) \rightarrow \; E_{ij} = \frac{1}{2}\left(F_{pi}F_{pj} - \delta_{ij}\right). \tag{6}$$

In the case of having principal stretches, invariants of the left Cauchy–Green strain tensor are:

$$\begin{aligned} I_1 &= \frac{\lambda_1^2 + \lambda_2^2 + \lambda_3^2}{\left(\lambda_1\lambda_2\lambda_3\right)^{\frac{2}{3}}}, \\ I_2 &= \frac{\lambda_1^2\lambda_2^2 + \lambda_1^2\lambda_3^2 + \lambda_2^2\lambda_3^2}{\left(\lambda_1\lambda_2\lambda_3\right)^{\frac{4}{3}}}, \\ I_3 &= \left(\lambda_1\lambda_2\lambda_3\right)^2. \end{aligned} \tag{7}$$

As for the hyperelasticity definition, a structure is hyperelastic if specific strain energy exists which is differentiable from the deformation gradient. In other words, to have a fully elastic behaviour, it is assumed that the strain energy density is directly dependent on the deformation gradient tensor. In another definition, it has been shown that a hyperelastic structure is isotropic if and only if the strain energy term can be rewritten via the three invariants of the left Cauchy–Green strain tensor [41].

According to Richter theorem [41, 42], the constitutive equation of an isotropic solid hyperelastic can be written as:

$$T = \beta_0 I + \beta_1 B + \beta_2 B^2, \tag{8}$$

if and only if the coefficients are defined following a specific relationship defined in the literature. It has been shown that [42], by having an isothermic process,

changes in $-T_0 dS$ (in which T_0 is the absolute temperature and S is the entropy) to become equal to the variation of the Helmholtz free energy. In case of isothermic process, coefficients in Eq. (8) are expressed by Eq. (9) as

$$\begin{aligned}\beta_0 &= \frac{\partial W}{\partial I_1} + I_1 \frac{\partial W}{\partial I_2} + I_2 \frac{\partial W}{\partial I_3},\\ \beta_1 &= -\frac{\partial W}{\partial I_2} - I_1 \frac{\partial W}{\partial I_3},\\ \beta_2 &= \frac{\partial W}{\partial I_3}.\end{aligned} \tag{9}$$

For a simple definition, by having the principal direction stretches, the normal stresses (σ_i) can be defined as [43]:

$$\sigma_i = \frac{\partial W}{\partial \lambda_i}, \quad i = 1,2,3 \tag{10}$$

after which, due to the definition of hyperelastic strain energy (W) being a function of its invariants, Eq. (10) can be rewritten as:

$$\frac{\partial W}{\partial \lambda_i} = \frac{\partial W}{\partial I_3}\frac{\partial I_3}{\partial \lambda_i} + \frac{\partial W}{\partial I_2}\frac{\partial I_2}{\partial \lambda_i} + \frac{\partial W}{\partial I_1}\frac{\partial I_1}{\partial \lambda_i}, \quad i = 1,2,3 \tag{11}$$

which for incompressible structures, the third term (derivation with respect to I_3) will be neglected. Different types of formulation and modelling for hyperelastic strain energy density have been presented in order to predict the nonlinear behaviour accurately. In further subsections, these isotropic models are presented and the formulation procedure for reaching the stress–strain equation is given. These models are used by many researchers to study the nonlinear dynamics of hyperelastic structures which is discussed in further sections.

2.2 The neo-Hookean model

This strain energy density expression is one of the straightforward models of a hyperelastic material in which we only consider the first and third invariant terms as

$$W_{NH} = \sum_{i=0}^{n} C_i \left(\overline{I_1} - 3\right)^i + D_1 (J-1)^2, \tag{12}$$

where W_{NH} is the strain energy density of this model, C_i are the coefficients of the first invariant parameter and D_1 is the compressibility factor, both of which must be obtained experimentally. For $n = 1$ (one-term neo-Hookean model), the axial stress (σ_{uni}) is written as [43]:

$$\begin{aligned}\sigma_{uni} = {} & C_1 \frac{4(1+v)}{3} \lambda_1^{-(5+2v)/3} \left(\lambda_1^{2+2v} - 1\right)\\ & + 2D_1(1-2v)\lambda_1^{-2v}(J-1),\end{aligned} \tag{13}$$

where v is the Poisson's ratio. By assuming an incompressible structure, Eq. (13) is simplified as:

$$\sigma_{uni} = 2C_1\left(\lambda - \lambda^{-2}\right), \tag{14}$$

and for equibiaxial (σ_{bi}) stress and pure shear (σ_s) stress, by using the same definition given in Eq. (12), the stress resultants become

$$\sigma_{bi} = 2C_1\left(\lambda - \lambda^{-5}\right), \tag{15}$$

$$\sigma_s = 2C_1\left(\lambda - \lambda^{-3}\right), \tag{16}$$

which coincides with those used in ref [44].

2.3 The Mooney–Rivlin model

One of the popular formulations and models used for predicting the hyperelastic behaviour of structures is the Mooney–Rivlin model [45], which is an extended form of the neo-Hookean model, considering the second invariant term. In the basic form, Mooney defined the strain energy density as a two-parameter model defined as:

$$W_M = C_1\left(\overline{I_1} - 3\right) + C_2\left(\overline{I_2} - 3\right) + D_1(J-1)^2, \tag{17}$$

where W_M is the strain energy density of the two-parameter Mooney model and C_i and D_1 are the coefficients that must be found via the experimental observations (such as the work done by Falope et al. [46] where the coefficients were calibrated using genetic algorithm), which can vary from one soft structure to another. Rivlin [47, 48] extended this equation by writing it in a general form as a polynomial series of the first and second invariant terms:

$$W_{MR} = \sum_{i=0}^{n}\sum_{j=0}^{m} C_{ij}\left(\overline{I_1} - 3\right)^i \left(\overline{I_2} - 3\right)^j + D_1(J-1)^2, \tag{18}$$

where W_{MR} is the strain energy density of the Mooney–Rivlin model, of which some of the well-known models and special cases of this polynomial series are the Biderman model [49], Klosner model [50] and Haines–Wilson model [51]. It has been mentioned already that this model has been widely used for analysing rubbers with less than 200% deformation [52].

For the two-parameter Mooney–Rivlin model under axial load, by having $\lambda_2 = \lambda_3 = \lambda_1^{-v}$, Brown et al. [43] obtained the axial stress as:

$$\sigma_{uni} = \frac{4(1+v)}{3}\lambda_1^{-(5+2v)/3}\left(\lambda_1^{2+2v}-1\right)\left(C_1 + C_2\lambda_1^{-2(1+v)/3}\right) + 2D_1(1-2v)\lambda_1^{-2v}(J-1), \tag{19}$$

from which, by assuming an incompressible structure, Eq. (19) becomes

$$\sigma_{uni} = 2C_1\left(\lambda - \lambda^{-2}\right) + 2C_2\left(1-\lambda^{-3}\right), \tag{20}$$

and for equibiaxial and pure shear stresses, by using the same definition given in Eq. (18), the stress resultants are:

$$\sigma_{bi} = 2C_1\left(\lambda - \lambda^{-5}\right) + 2C_2\left(\lambda^3 - \lambda^{-3}\right), \tag{21}$$

$$\sigma_s = (2C_1 + 2C_2)\left(\lambda - \lambda^{-3}\right), \tag{22}$$

which coincides with those used in ref [44]. To have a better understanding of the Mooney–Rivlin model, the effect of the coefficients C_1 and C_2 on the uniaxial stress is presented in Fig. 5 for axial strain up to 100%. It can be seen that the stress–strain behaviour is completely nonlinear and the curve model is highly sensitive to the two-parameter Mooney–Rivlin coefficients. By having [37] $C_1 = 0.39$ MPa and $C_2 = 0.015$ MPa, in Fig. 5a, the first coefficient term is varied as $[0.5C_1–1.5C_1]$, while in Fig. 5b the second coefficient is varied as $[0.5C_2–5.5C_2]$. Since the formulation of a neo-Hookean model is somewhat similar to the Mooney–Rivlin hyperelastic model (by neglecting the second invariant term), the influence of varying the hyperelastic coefficient C_1 in one-term neo-Hookean models will be very similar to the one presented in Fig. 5a.

2.4 The Ogden model

Ogden [53, 54] proposed a series of models of strain energy density as a direct function of principal stretches

$$W_{Og} = \sum_{i=1}^{n}\frac{2\mu_i}{\alpha_i^2}\left(\lambda_1^{\alpha_i} + \lambda_2^{\alpha_i} + \lambda_3^{\alpha_i} - 3\right) + \sum_{i=1}^{n} D_i(J-1)^{2i} \tag{23}$$

where W_{Og} is the strain energy density of the Ogden model and μ_i, D_i and α_i are the constant properties that must be found using experimental testing. This model is well capable of simulating the typical hardening of rubber materials, which is not included in both neo-

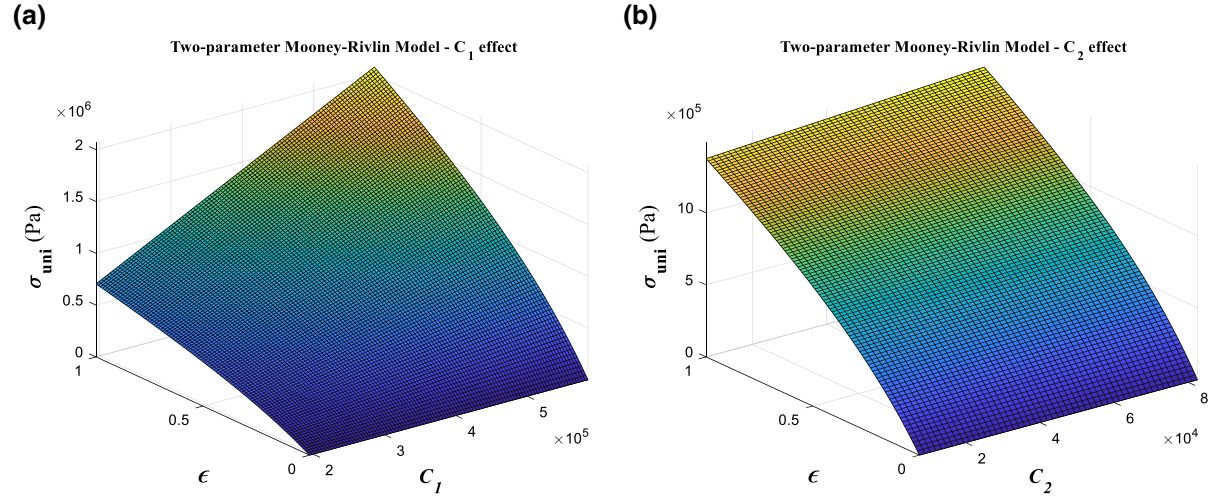

Fig. 5 Uniaxial stress sensitivity to the *two-parameter Mooney–Rivlin* coefficients: **a** C_1; **b** C_2

Hookean and Mooney–Rivlin models. Brown et al. [43] have shown the uniaxial stress for this model to be:

$$\sigma_{uni} = \sum_{i=1}^{n} \frac{2\mu_i}{\alpha_i}\left(\lambda^{\alpha_i-1} - 2v\lambda^{-\alpha_i v-1}\right) + 2\left(1-2v\lambda^{-2v}\right)\sum_{i=1}^{n} iD_i(J-1)^{2i-1} \tag{24}$$

which can be rewritten for incompressible structures as

$$\sigma_{uni} = \sum_{i=1}^{n} \frac{2\mu_i}{\alpha_i^2}\left(\lambda^{\alpha_i-1} - \lambda^{-\frac{\alpha_i}{2}-1}\right). \tag{25}$$

Similarly, the equibiaxial and pure shear stresses are:

$$\sigma_{bi} = \sum_{i=1}^{n} \frac{2\mu_i}{\alpha_i^2}\left(\lambda^{\alpha_i-1} - \lambda^{-2\alpha_i-1}\right), \tag{26}$$

$$\sigma_s = \sum_{i=1}^{n} \frac{2\mu_i}{\alpha_i^2}\left(\lambda^{\alpha_i-1} - \lambda^{-\alpha_i-1}\right). \tag{27}$$

In order to elaborate the impact of each coefficient term on the stress–strain behaviour of Ogden hyperelastic models, uniaxial loading of a three-parameter Ogden model is considered with coefficients and power terms as [37], where $\mu_1 = 0.62$ MPa, $\mu_2 = 0.00118$ MPa, $\mu_3 = 0.00981$ MPa, $\alpha_1 = 1.3$, $\alpha_2 = 5$ and $\alpha_3 = -2$. Figures 6a–f indicate the strong effect of varying three-parameter Ogden model coefficients and power terms by [0.5 μ_1–1.5 μ_1], [0.5α_1–1.5α_1], [0.5μ_2–50.5μ_2], [0.5 α_2–15.5α_2], [0.5μ_3–5.5μ_3] and [0.5α_3–15.5α_3], respectively. It can be seen that each parameter has its own effect on the axial stress magnitude through which, by properly accounting for these terms, the hyperelastic behaviour of rubbery structures can be obtained.

2.5 The eight-chain (Arruda–Boyce) model

Arruda and Boyce [55] proposed the eight-chain model in which the strain energy is described as a function of a polynomial series of the first invariant as

$$W_{AB} = \sum_{i=1}^{n} C_i\left(\overline{I_1^i} - 3^i\right) + \sum_{i=1}^{n} D_i(J-1)^{2i}, \tag{28}$$

where W_{AB} is the strain energy density of the Arruda–Boyce model, for which, under uniaxial loading, the stress-stretch equation will become [43]

$$\sigma_{uni} = \frac{4(1+v)}{3}\sum_{i=1}^{n} iC_i\left(\overline{I_1^{i-1}}\right)\lambda^{-(5+2v)/3}\left(\lambda^{2+2v}-1\right) + 2(1-2v)\sum_{i=1}^{n} iD_i(J-1)^{2i-1}\lambda^{-2v}, \tag{29}$$

which for incompressible structures it is simplified as

$$\sigma_{uni} = 2\sum_{i=1}^{n} iC_i\left(\overline{I_1^{i-1}}\right)\left(\lambda - \lambda^{-2}\right), \tag{30}$$

with equibiaxial and pure shear stresses as

$$\sigma_{bi} = 2\sum_{i=1}^{n} iC_i\left(\overline{I_1^{i-1}}\right)\left(\lambda - \lambda^{-5}\right), \tag{31}$$

$$\sigma_s = 2\sum_{i=1}^{n} iC_i\left(\overline{I_1^{i-1}}\right)\left(\lambda - \lambda^{-3}\right). \tag{32}$$

For analysing the coefficient sensitivity of this model, a five-parameter Arruda–Boyce model is considered by having [56] $C_1 = \mu/2$, $C_2 = \mu/20$, $C_3 = 11\mu/1050$, $C_4 = 19\mu/7000$, $C_5 = 519\mu/673750$ where μ is the rubbery shear modulus assumed to be 0.4 MPa. The influence of each coefficient on the uniaxial stress variation can be seen in Fig. 7a–f by varying [0.5μ–1.5μ], [0.5C_1–1.5C_1], [0.5C_2–2C_2], [0.5C_3–2.5C_3], [0.5C_4–5C_4], and [0.5C_5–5C_5], respectively. Here, all the coefficients have a considerable effect on the uniaxial stress term.

2.6 The polynomial model

The strain energy in the polynomial rubber model is defined as [57]

$$W_{Po} = \sum_{i+j=1}^{n} C_{ij}\left(\overline{I_1}-3\right)^i\left(\overline{I_2}-3\right)^j + \sum_{i=1}^{n} D_i(J-1)^{2i}, \tag{33}$$

where W_{Po} is the strain energy density of polynomial model, which can also be written as [43]

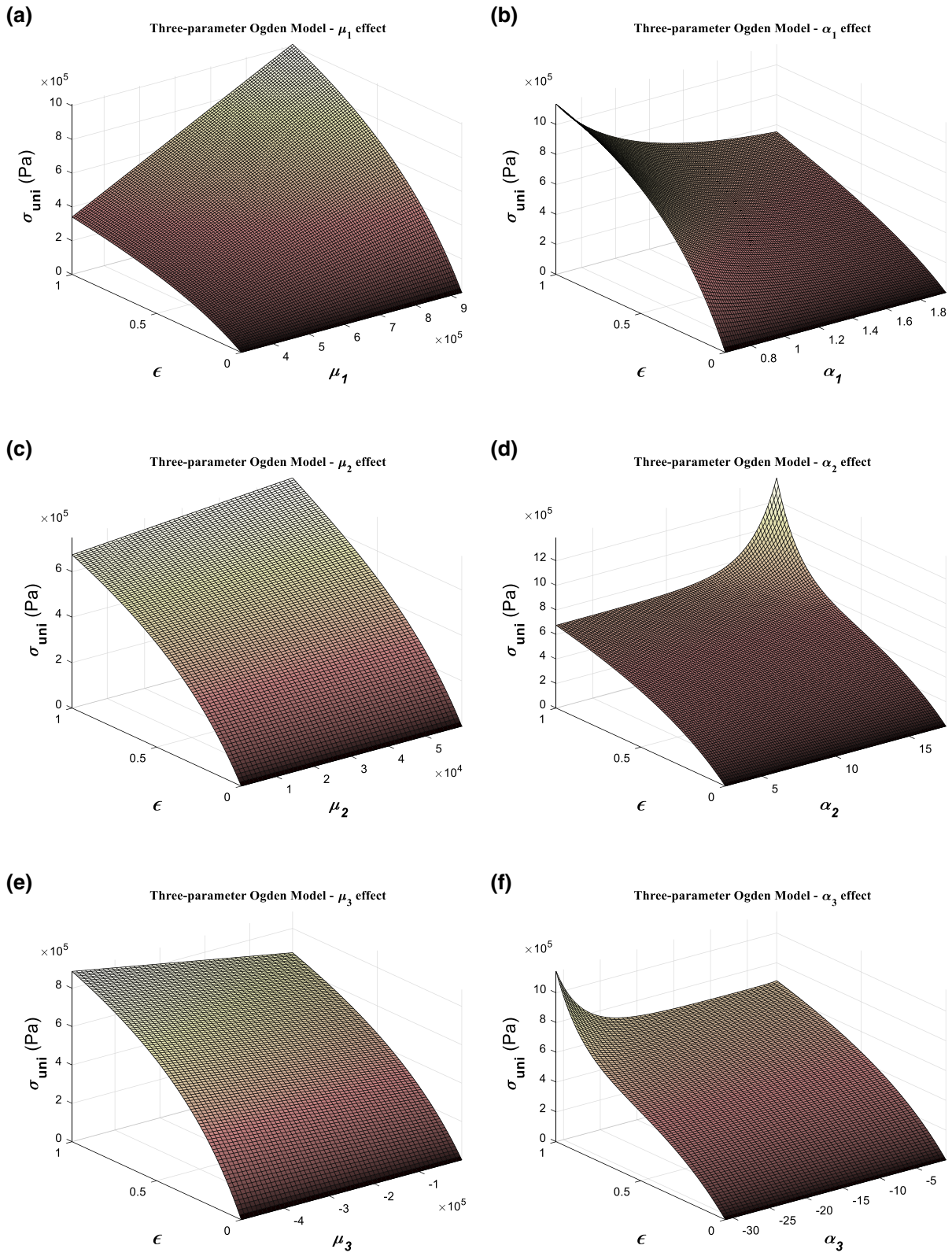
(a)
Three-parameter Ogden Model - μ_1 effect
σ_{uni} (Pa)
ϵ
μ_1
(b)
Three-parameter Ogden Model - α_1 effect
σ_{uni} (Pa)
ϵ
α_1
(c)
Three-parameter Ogden Model - μ_2 effect
σ_{uni} (Pa)
ϵ
μ_2
(d)
Three-parameter Ogden Model - α_2 effect
σ_{uni} (Pa)
ϵ
α_2
(e)
Three-parameter Ogden Model - μ_3 effect
σ_{uni} (Pa)
ϵ
μ_3
(f)
Three-parameter Ogden Model - α_3 effect
σ_{uni} (Pa)
ϵ
α_3

◀ **Fig. 6** Uniaxial stress sensitivity to the *three-parameter Ogden* coefficients and power terms: **a** μ_1; **b** α_1; **c** μ_2; **d** α_2; **e** μ_3; **f** α_3

$$W_{Po} = \sum_{i=0}^{n} \sum_{j=1-i}^{n-i} C_{ij} \left(\overline{I}_1 - 3\right)^i \left(\overline{I}_2 - 3\right)^j + \sum_{i=1}^{n} D_i (J-1)^{2i}, \tag{34}$$

leading to an axial stress–stretch relationship as [43]

$$\sigma_{uni} = \frac{4(1+\nu)}{3} \lambda^{-(5+2\nu)/3} \left(\lambda^{2+2\nu} - 1\right) \left[\begin{array}{l} \sum_{i=0}^{n} \sum_{j=1-i}^{n-i} iC_{ij} \left(\overline{I}_1 - 3\right)^{i-1} \left(\overline{I}_2 - 3\right)^j \\ +\lambda^{-(2+2\nu)/3} \sum_{i=0}^{n} \sum_{j=1-i}^{n-i} jC_{ij} \left(\overline{I}_1 - 3\right)^i \left(\overline{I}_2 - 3\right)^{j-1} \end{array} \right] + 2(1-2\nu) \sum_{i=1}^{n} iD_i (J-1)^{2i-1} \lambda^{-2\nu}, \tag{35}$$

which, for incompressible structures using Eq. (33), is rewritten as

$$\sigma_{uni} = 2 \sum_{i=0}^{n} \sum_{j=1-i}^{n-i} iC_{ij} \left(\overline{I}_1 - 3\right)^{i-1} \left(\overline{I}_2 - 3\right)^j \left(\lambda - \lambda^{-2}\right) + 2 \sum_{i=0}^{n} \sum_{j=1-i}^{n-i} jC_{ij} \left(\overline{I}_1 - 3\right)^i \left(\overline{I}_2 - 3\right)^{j-1} \left(1 - \lambda^{-3}\right), \tag{36}$$

and for equibiaxial and pure shear stresses as

$$\sigma_{bi} = 2 \sum_{i=0}^{n} \sum_{j=1-i}^{n-i} iC_{ij} \left(\overline{I}_1 - 3\right)^{i-1} \left(\overline{I}_2 - 3\right)^j \left(\lambda - \lambda^5\right) + 2 \sum_{i=0}^{n} \sum_{j=1-i}^{n-i} jC_{ij} \left(\overline{I}_1 - 3\right)^i \left(\overline{I}_2 - 3\right)^{j-1} \left(\lambda^3 - \lambda^{-3}\right), \tag{37}$$

$$\sigma_s = 2\left(\lambda - \lambda^{-3}\right) \left[\begin{array}{l} \sum_{i=0}^{n} \sum_{j=1-i}^{n-i} iC_{ij} \left(\overline{I}_1 - 3\right)^{i-1} \left(\overline{I}_2 - 3\right)^j \\ +\sum_{i=0}^{n} \sum_{j=1-i}^{n-i} jC_{ij} \left(\overline{I}_1 - 3\right)^i \left(\overline{I}_2 - 3\right)^{j-1} \end{array} \right]. \tag{38}$$

Similar to the previous subsections, by assuming the coefficients to be $C_{10} = 1.44$ MPa, $C_{01} = 0.463$ MPa, $C_{11} = -0.029$ MPa, $C_{20} = -0.151$ MPa, and $C_{02} = -0.0042$ MPa, Fig. 8a–f present the influence of varying the coefficients of the five-parameter polynomial model on the axial stress for strains up to 100%. Coefficients are assumed to vary as $[0.5C_{10}$–$1.5C_{10}]$, $[0.5C_{01}$–$1.5C_{01}]$, $[0.5C_{11}$–$1.5C_{11}]$, $[0.5C_{20}$–$1.5C_{20}]$ and $[0.5C_{20}$–$3C_{02}]$, respectively.

2.7 The Gent model

Gent [57, 58] proposed a simple model of hyperelasticity using the first invariant parameter:

$$W_G = -\frac{\mu}{2} J_m \ln\left(1 + \frac{3 - I_1}{J_m}\right), \tag{39}$$

where W_G is the strain energy density of the Gent model and J_m is the limiting stretch parameter [59], which for biological tissues is around (0.4–2.3) [60–63] and for plastic structures is in orders of 100 [57, 58]. By increasing the maximum permitted value J_m to infinity, the Gent model will be changed to the neo-Hookean incompressible model. The uniaxial, biaxial and pure shear stresses for this model will be

$$\sigma_{uni} = \mu J_m \left(\lambda - \frac{1}{\lambda^2}\right) \left(1 + \frac{3 - I_1}{J_m}\right)^{-1}, \tag{40}$$

$$\sigma_{bi} = 2\mu J_m \left(\lambda - \frac{1}{\lambda^5}\right) \left(1 + \frac{3 - I_1}{J_m}\right)^{-1}, \tag{41}$$

$$\sigma_s = \mu J_m \left(\lambda - \frac{1}{\lambda^3}\right) \left(1 + \frac{3 - I_1}{J_m}\right)^{-1}, \tag{42}$$

of which Eq. (40) coincides with the uniaxial stress model presented by Ronald [64]. Figure 9a shows the sensitivity of the axial stress parameter to variations of μ for $J_m = 5$ and Fig. 9b shows the sensitivity of the axial stress parameter to variations of J_m for $\mu = 0.4$ MPa. Although the main model presented by Gent is only dependent on the first invariant, modified versions of this model, designed to incorporate the compressibility and other invariant terms, have been extended by several researchers [65–68].

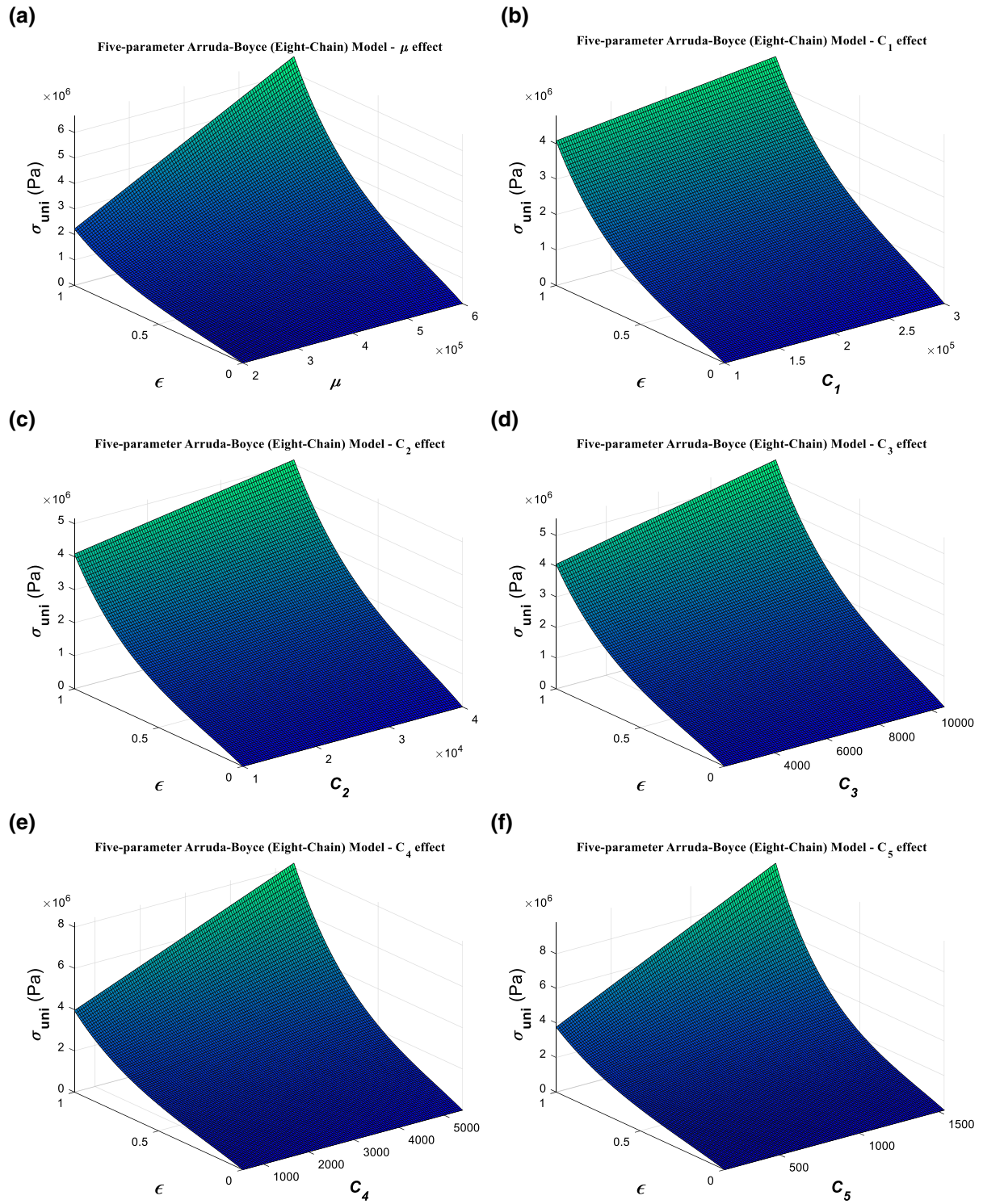

Fig. 7 Uniaxial stress sensitivity to the *five-parameter Arruda–Boyce* (eight-chain) model coefficients: **a** μ; **b** C_1; **c** C_2; **d** C_3; **e** C_4; **f** C_5

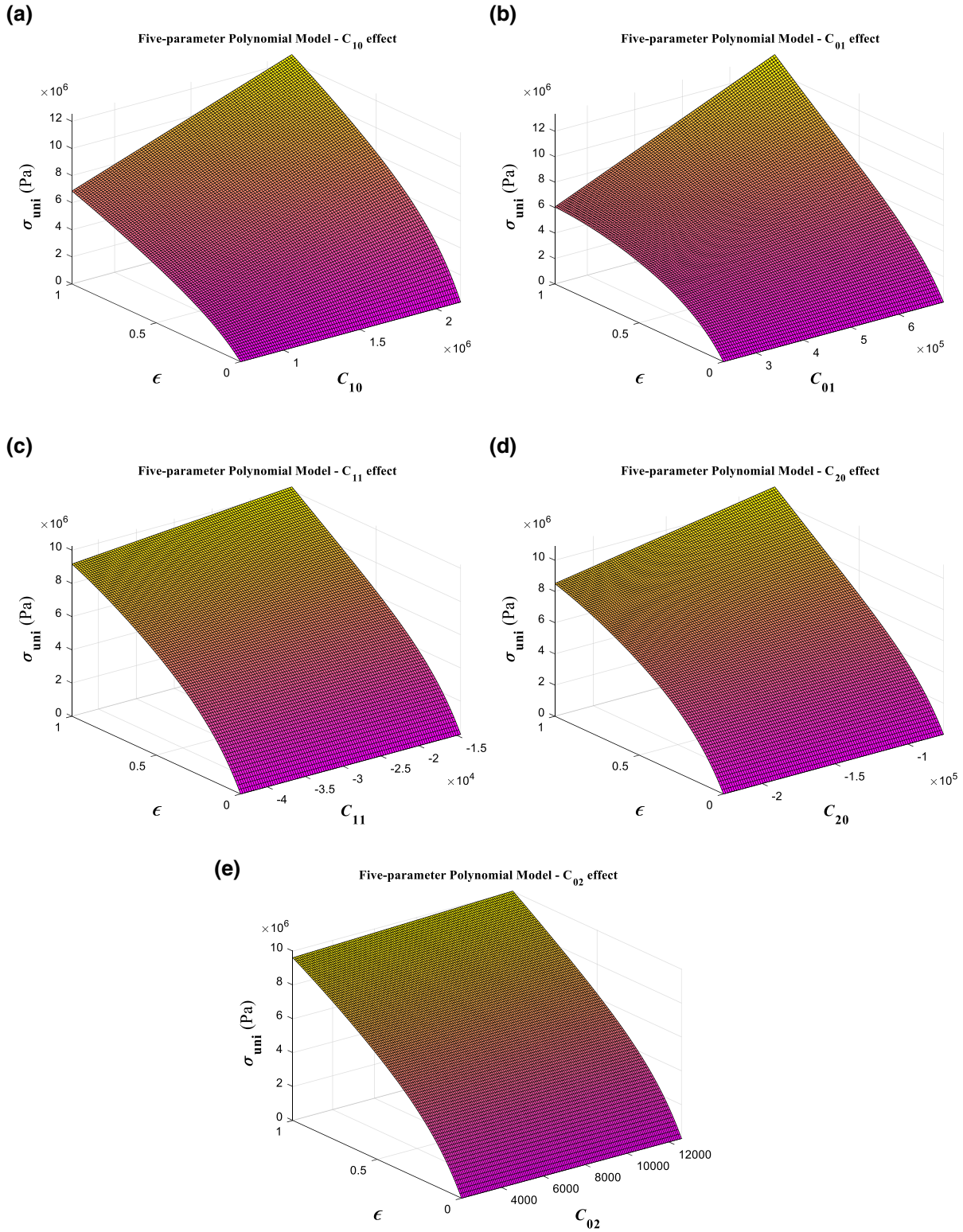

Fig. 8 Uniaxial stress sensitivity to the *five-parameter polynomial* model coefficients: **a** C_{10}; **b** C_{01}; **c** C_{11}; **d** C_{20}; **e** C_{02}

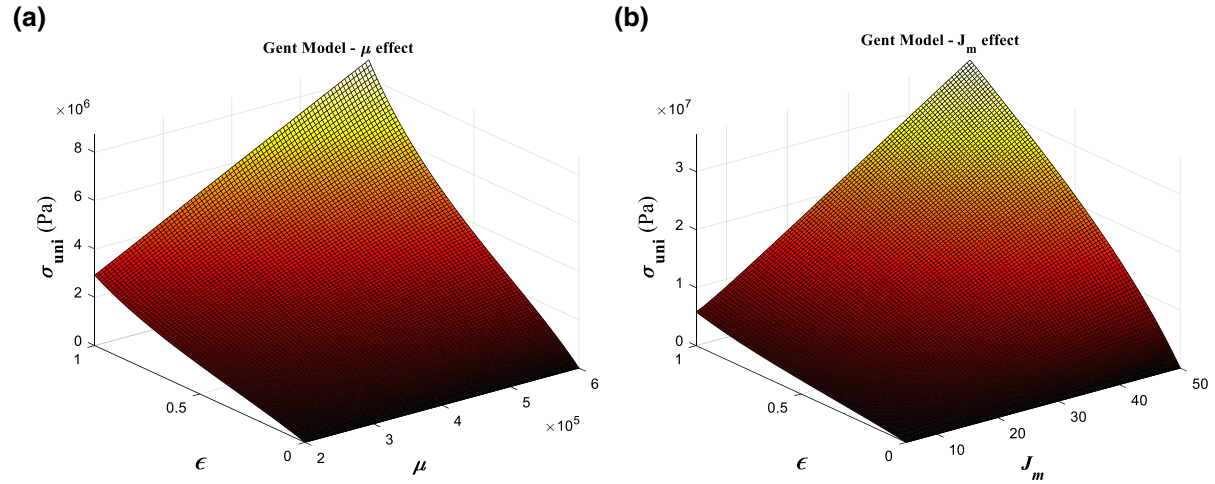

Fig. 9 Uniaxial stress sensitivity to the *Gent* model coefficients: **a** μ; **b** J_m

2.8 The Blatz–Ko model

For the proposed model by Blatz and Ko [69], which is used to characterise foam rubbery structures, the strain energy density is written as [43]:

$$W_{BK} = \frac{\mu}{2}\left(\frac{I_1}{I_2} + 2\sqrt{I_3}\right), \tag{43}$$

where W_{BK} is the Blatz–Ko model of the strain energy density and for the incompressible structures, for axial loading, equibiaxial and pure shear stresses the stress–stretch relationship is, respectively, obtained as:

$$\sigma_{uni} = \frac{\mu}{2\lambda + \lambda^{-2}}\left[\left(\lambda - \lambda^{-2}\right) + \frac{\left(\lambda^2 + 2\lambda^{-1}\right)}{\left(2\lambda + \lambda^{-2}\right)}\left(1 - \lambda^{-3}\right)\right], \tag{44}$$

$$\sigma_{bi} = \frac{\mu}{2\lambda + \lambda^{-2}}\left[\left(\lambda - \lambda^{-5}\right) + \frac{\left(\lambda^2 + 2\lambda^{-1}\right)}{\left(2\lambda + \lambda^{-2}\right)}\left(\lambda^3 - \lambda^{-3}\right)\right], \tag{45}$$

$$\sigma_s = \frac{\mu}{2\lambda + \lambda^{-2}}\left(\lambda - \lambda^{-3}\right)\left[1 + \frac{\left(\lambda^2 + 2\lambda^{-1}\right)}{\left(2\lambda + \lambda^{-2}\right)}\right]. \tag{46}$$

Figure 10 presents the influence of varying the Blatz–Ko coefficient on the nonlinear stress–strain behaviour of uniaxial loaded structures. There are many other models presented by researchers to model the hyperelastic behaviour of such structures [41], such as the Rivlin–Saunders model [41], the Murnaghan model [70], the Ciarlet model [71], the Valanis–Landel model [72], the Hill model [73] and the Attard model [74].

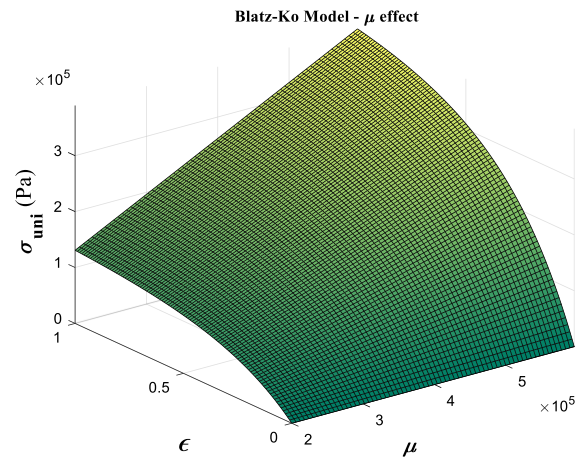

Fig. 10 Uniaxial stress sensitivity to the *Blatz–Ko* model coefficient

The given models are mainly used for isotropic hyperelastic materials; however, some structures (especially biological tissues) show a more complicated behaviour which requires orthotropic and anisotropic modelling in their hyperelastic constitutive models. These models are developed mainly for a specific type of hyperelastic materials. A more detailed explanation on orthotropic and anisotropic modelling can be found in refs [75–80] and [81–90], respectively.

An important topic in hyperelasticity analysis is properly modelling the nonlinear dynamics of different soft structures. Since hyperelastic structures have been used lately in many different industrial needs

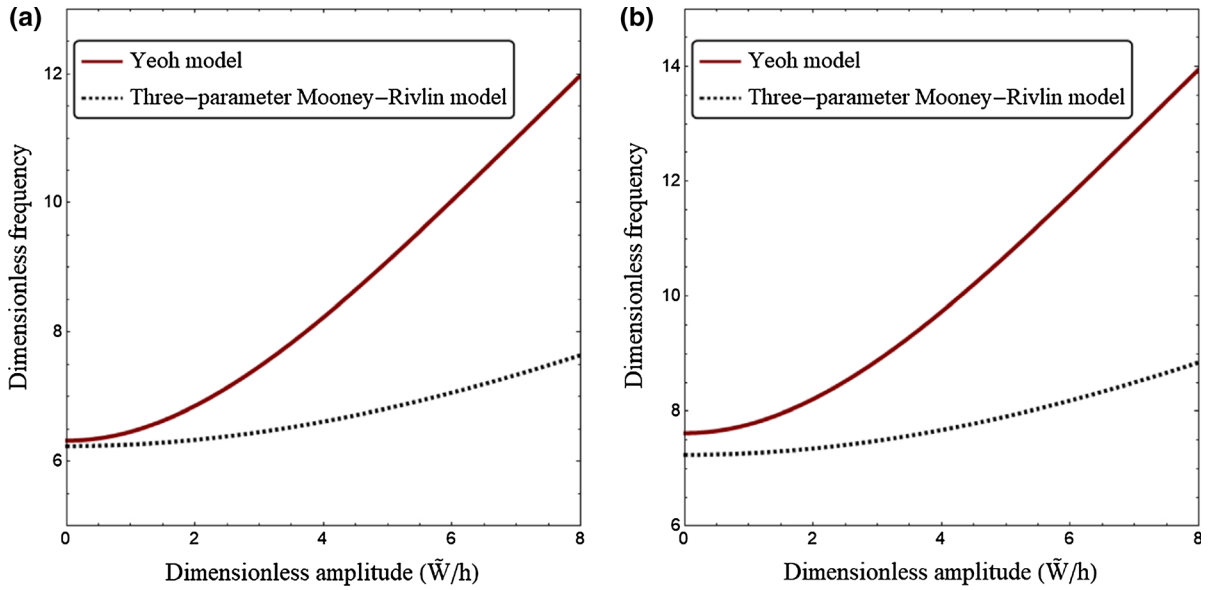

Fig. 11 The nonlinear frequencies of hyperelastic tube models using Yeoh and Mooney–Rivlin strain energy density models for **a** pinned–pinned and **b** clamped–clamped boundary conditions [106]. (Permission obtained from Springer Nature)

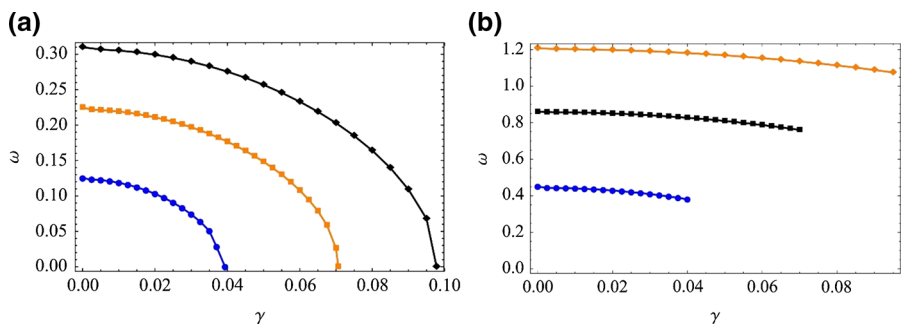

Fig. 12 Variation of the **a** first and **b** second natural frequencies of neo-Hookean axially moving beams with respect to the velocity parameter for different geometrical parameters [109]. (Permission obtained from ELSEVIER)

such as soft robotics [91–94], understanding their nonlinear time-dependant behaviour in different mechanical conditions is of high importance. Studies in this field can be classified based on the structure type and the mechanical analysis. In this review, the nonlinear dynamics of hyperelastic structures is presented in three sections for beams, plates/shells and membranes/balloons.

3 Nonlinear dynamics of hyperelastic beams

One-dimensional structures, including beams, tubes and columns, as the critical part of many mechanical structures, undergo different types of dynamic loads. Since rubber-like beams undergo large strains and deformations, classical linear material models cannot define the nonlinear dynamics accurately; therefore, an accurate hyperelastic model of the structure should be derived and examined. In this section, the nonlinear dynamics of hyperelastic beams is reviewed using literature for different mechanical conditions. Since this review is focused on the nonlinear dynamics, interested readers on the statics of hyperelastic beam structures are referred to [17, 95–100].

For hyperelastic beams laying on a foundation, a mathematical formulation was presented by Forsat [101] to examine the nonlinear free vibration behaviour of silicone rubbers and natural rubbers. A higher-order shear deformation beam theory together with four different nonlinear elasticity models was utilised for modelling the soft beam. The structure was assumed to be sitting on a Pasternak–Winkler medium. Equations of motion were solved and

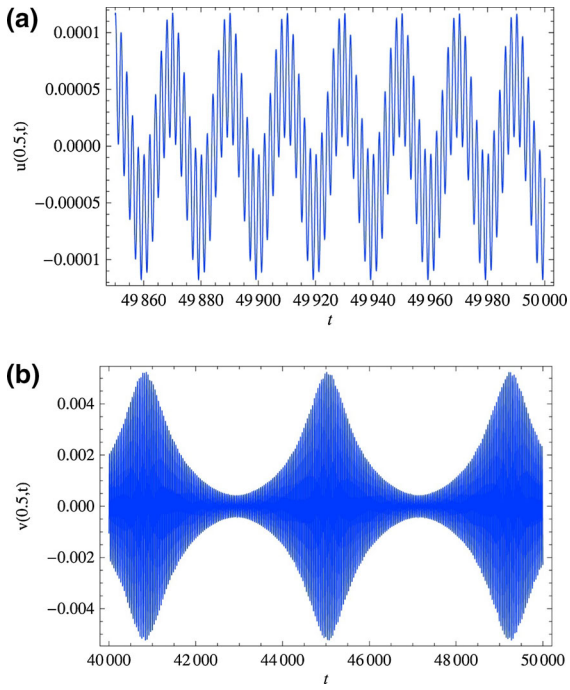

Fig. 13 The time traces for the **a** axial and **b** transverse vibrations of axially accelerated neo-Hookean beams [112]. (Permission obtained from ELSEVIER)

obtained using Galerkin's scheme and Hamilton's principle (which have been used by researchers for studying elastic structures [102–105]), respectively; it was claimed that the shear strain effects were neglected in the Yeoh strain energy. In another study, Mirjavadi et al. [106] used the Euler–Bernoulli beam assumptions showing that for hyperelastic tube models, by increasing the amplitude of vibration, since the effect of nonlinear terms in the structure modelling increases and due to different stress invariant considerations, the difference between the Yeoh and two-parameter Mooney–Rivlin results increased. Figure 11 shows the nonlinear frequencies of hyperelastic tube models using Yeoh and Mooney–Rivlin strain energy density models. In both of these studies, the material was assumed to be incompressible; however, the incompressibility condition, which leads to strains in thickness directions, was neglected.

Since belt operating systems are one of the well-known applications of hyperelastic structures [107, 108], researchers focused on the nonlinear dynamics of axially moving hyperelastic beams to understand their mechanical behaviour in such conditions. Wang et al. [109] used a finite deformation leading-order model (presented in [110, 111]) to investigate the nonlinear oscillations of axially travelling soft beams. Using the Hamilton's principle and neo-Hookean strain energy density model, the equations of motion were obtained. It was claimed that the natural frequencies of the Euler–Bernoulli beam model are lower than the ones obtained for this model. The variation of the natural frequencies with respect to the axial velocity parameter for this model is shown in Fig. 12. In another study by Wang et al. [112], they analysed accelerated longitudinal motion in soft beams using multiple scale perturbation methods and Galerkin's scheme. The time traces for the axial and transverse vibrations of this model are shown in Fig. 13. Khaniki et al. [113] investigated the nonlinear forced oscillation of axially moving hyperelastic belts by employing the Yeoh's strain energy. Different nonlinear elastic models were examined to find the best fit with the experimental testing of hyperelastic properties. The influence of the longitudinal speed on the natural frequencies, mode shapes and nonlinear frequency response was investigated showing a significant effect in changing the mechanical behaviour (Figs. 14 and 15).

For the case of having both thermal and hyperelasticity effects, a wave propagation method was employed by Mirparizi and Fotuhi [114] to understand the nonlinear dynamics of thermo-hyperelastic one-dimensional structures. Hyperelasticity was modelled using a Mooney–Rivlin strain energy density model. It was elucidated that the maximum amplitude of oscillation in the structure is significantly higher than for elastic ones. Figure 16 shows the stress wave propagation with respect to time showing a large difference between the hyperelastic and linear elastic models response.

Since hyperelastic structures are mostly made by moulding and 3D printing, the presence of voids and porosity is highly possible. To understand the effect of having porosities in the nonlinear dynamics of hyperelastic structures, Khaniki et al. [115] studied the characteristics of hyperelastic samples experimentally with different porosities (the infill rate). A general constitutive model for hyperelastic-porous was presented via the Mooney–Rivlin hyperelastic strain energy model, showing that the porosity has a nonlinear effect in varying the hyperelastic constitutive model (Fig. 17). For the derived model, they modelled the nonlinear vibrations of porous

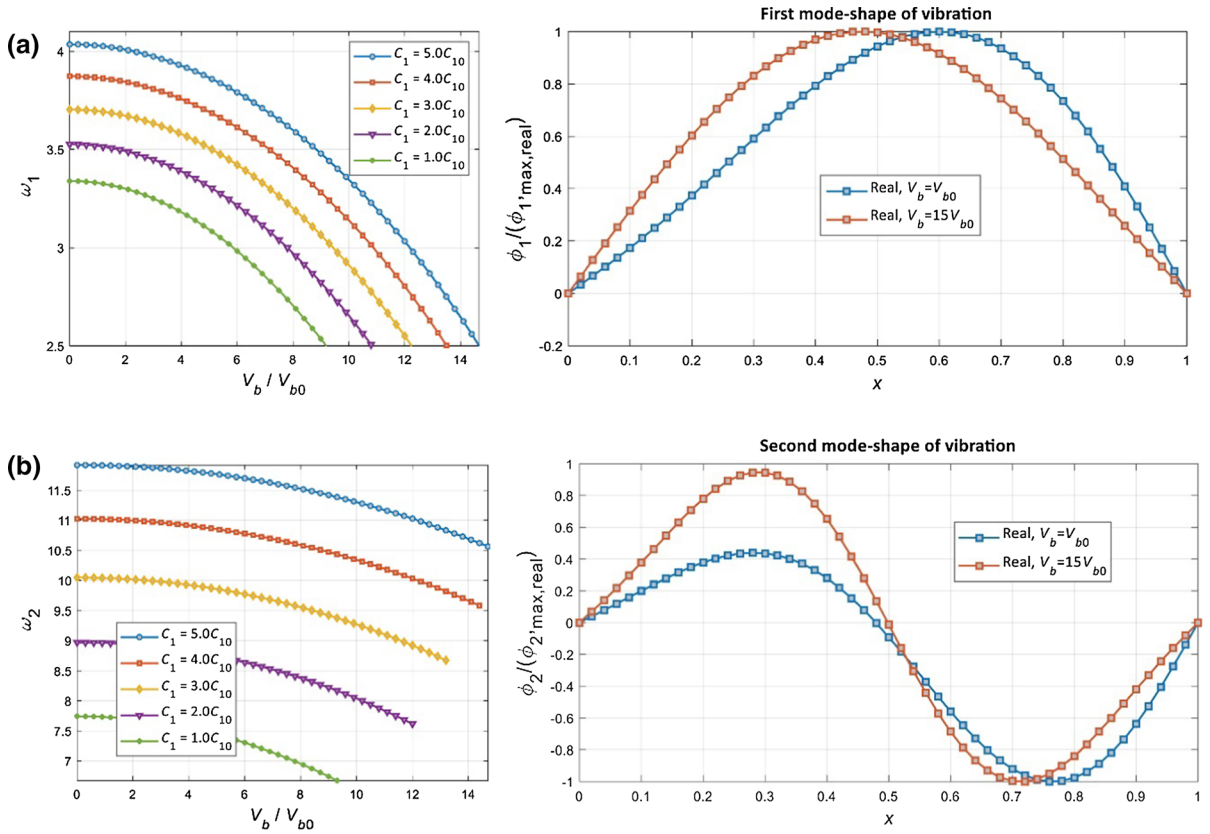

Fig. 14 The natural frequency and mode shapes of axially moving hyperelastic beams versus the speed parameter **a** first and **b** second modes of vibration [113]. (Permission obtained from ELSEVIER)

hyperelastic beams under externally time-dependent forces, showing that increasing the porosity in the structure has a significant effect in changing the stiffness softening behaviour of the structure to a combination of hardening and softening behaviour (Fig. 18).

Layered hyperelastic structures have many applications in packaging industry (especially food packaging) [116–119], which makes it important to comprehend the behaviour of layered hyperelastic structures made of different materials. For this reason, Khaniki et al. [120] examined five different shear deformable beam theories together with the Mooney–Rivlin strain energy model for analysing the nonlinear dynamics of sandwich soft beams. It was shown that considering the shear effect, layering and material positioning can highly affect the nonlinear resonance behaviour of the thick sandwich soft beam. Figure 19 shows the effect of material ordering in changing the nonlinear dynamic behaviour of higher-order shear deformable three-layered beam structures.

Longitudinal vibrations of neo-Hookean beams have been examined by Wang and Zhu [121, 122] in its subcritical buckling regime and under different axial loads. Using a linear bifurcation analysis, the critical buckling loads were obtained showing a high sensitivity of material and geometrical properties. Using the pseudo-arc-length method, the nonlinear frequency response of the system was calculated. Figure 20 shows the axial frequency response of the neo-Hookean beam model for different material and geometrical properties.

In recent years, hyperelasticity has been employed for modelling the static and dynamic responses of

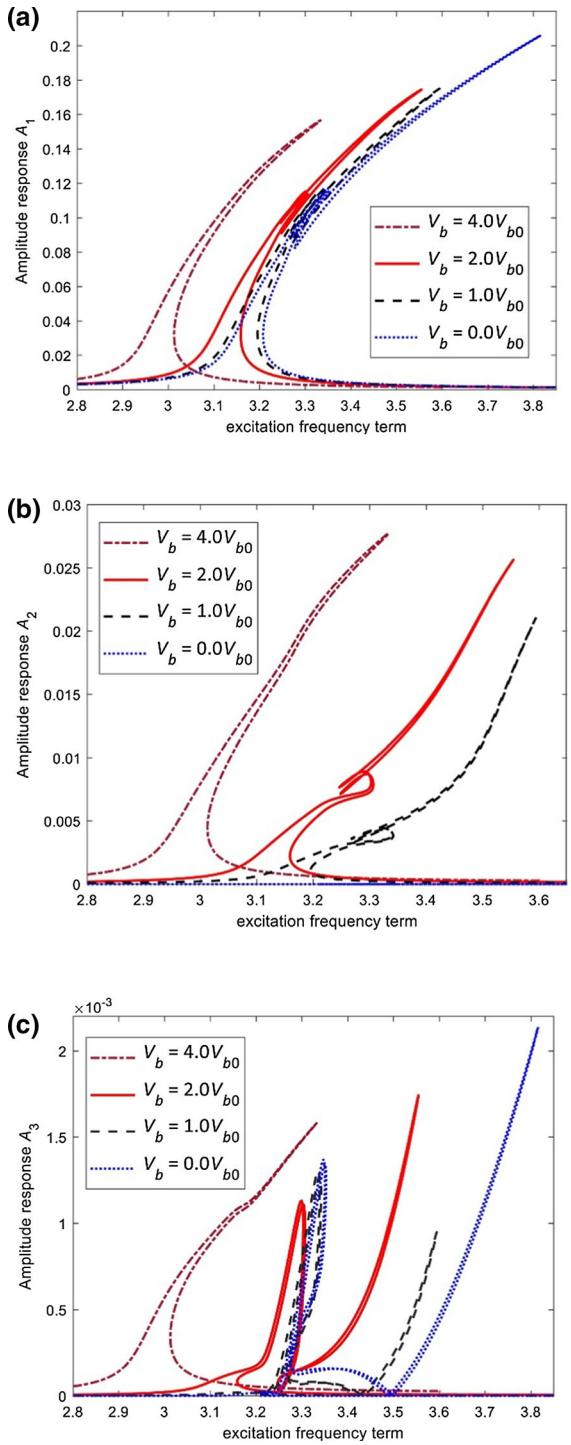

Fig. 15 The transverse amplitude–frequency response of axially moving hyperelastic beams with different velocities **a** first, **b** second, and **c** third coordinates [113]. (Permission obtained from ELSEVIER)

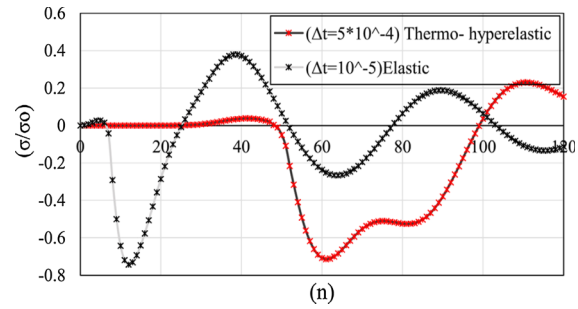

Fig. 16 Stress wave propagation in hyperelastic and elastic structures [114]. (Permission obtained from ELSEVIER)

nano-/micromaterials [123–126], which have crucial importance in new technologies. For instance, micro-scale beam structures made by hyperelastic materials have been studied by Alibakhshi et al. [127] using the Euler–Bernoulli beam theory, modified couple stress theory (which have been used previously for studying small-scale elastic structures [128–132]), and Gent strain energy density model. It was shown that the force–amplitude response of the structure is highly sensitive to the stiffness parameter of Gent model (Fig. 21). Studies on the nonlinear dynamics of hyperelastic beams are summarised in Table 1.

4 Nonlinear dynamics of hyperelastic plates and shells

Both shells and plates are an important element in structural design, and the extensive usage of rubbery structures makes it necessary to comprehend the nonlinear dynamics of the hyperelastic plate and shell structures. For this reason, this section focuses on the investigations undertaken to comprehend the nonlinear dynamics of such structures.

For isotropic hyperelastic plate structures, a combination of the nonlinear von Kármán plate theory and the neo-Hookean strain energy density model was used by Breslavsky et al. [133] for examining the large amplitude vibrations of thin rectangular hyperelastic plates. The equations of motion were presented with quadratic and cubic nonlinear terms by considering both material and geometrical nonlinearities; it was shown that for small strains, the material nonlinearity terms have a weak effect, while this effect increases significantly by having larger strains. Figure 22 shows the amplitude response and backbone curves of the

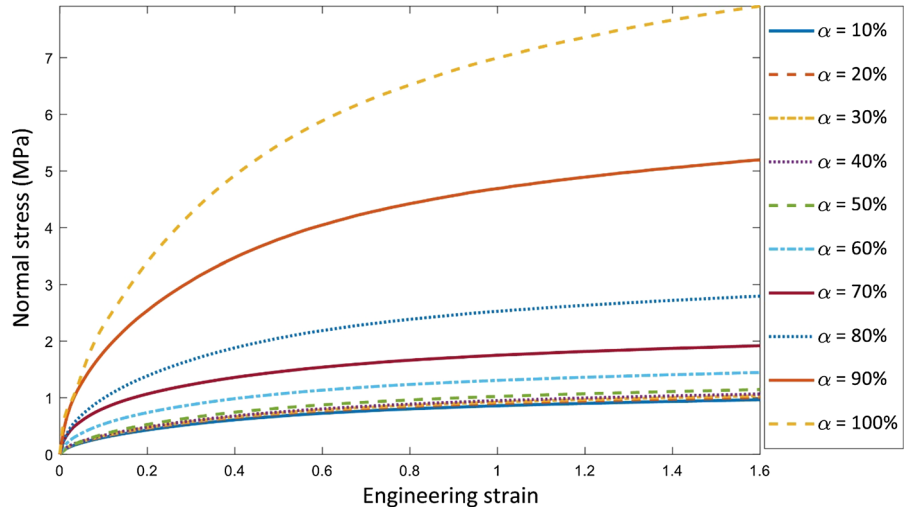

Fig. 17 Experimental results for stress–strain behaviours of porous hyperelastic structures with different infill rates (α) [115]. (Permission obtained from ELSEVIER)

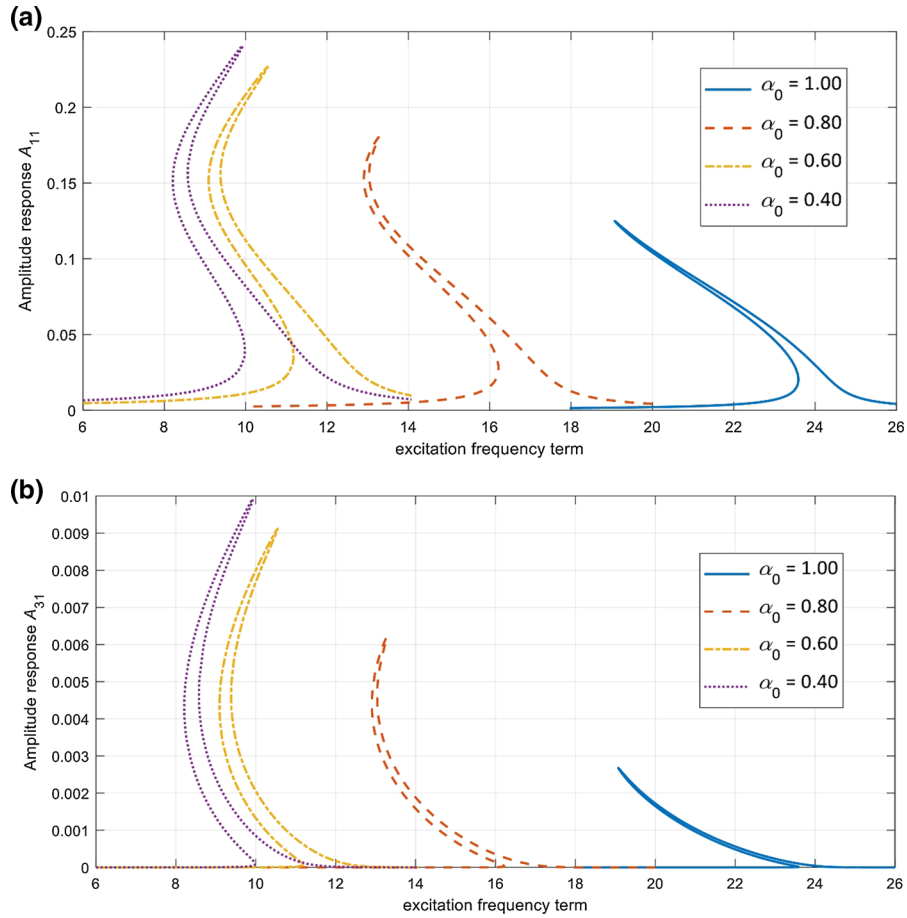

Fig. 18 Influence of the infill rate (porosity) in varying the nonlinear frequency response of porous hyperelastic beams **a** first and **b** third dynamic coordinates. [115]. (Permission obtained from ELSEVIER)

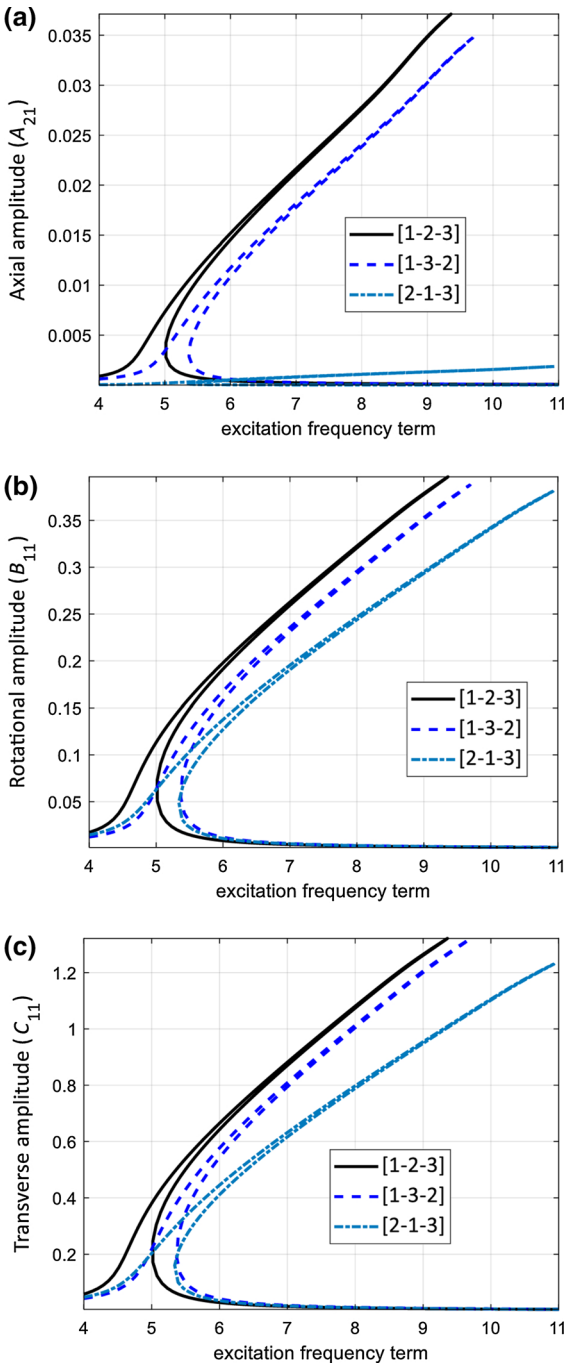

Fig. 19 The effect of hyperelastic material layering on the nonlinear dynamics Mooney–Rivlin shear deformable beams for the **a** axial, **b** rotational and **c** transverse motions [120]. (This article is an open access article distributed under the terms and conditions of the Creative Commons Attribution (CC BY) license (https://creativecommons.org/licenses/by/4.0/).)

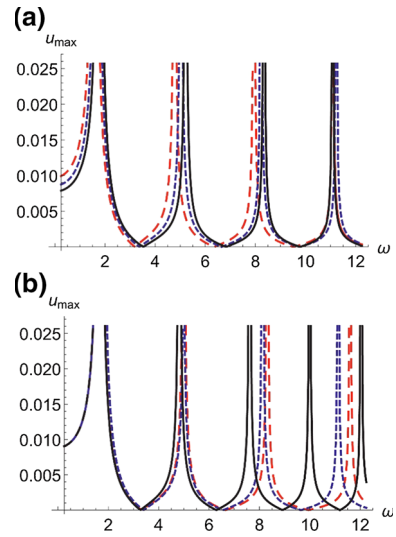

Fig. 20 The axial nonlinear frequency response of the neo-Hookean beam model for different **a** material and **b** geometrical properties [121]. (Permission obtained from ELSEVIER)

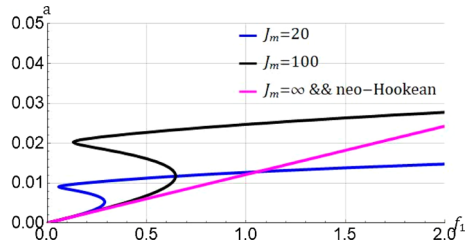

Fig. 21 The force–amplitude response of micro-hyperelastic beam for different Gent coefficients[127]. (Permission obtained from MDPI)

first mode of vibration with two peaks associated with the 2:1 in-plane resonance. Amabili et al. [134] investigated the vibration behaviour of hyperelastic plates. A two-parameter incompressible Mooney–Rivlin model was used to describe the nonlinearity of the structure using Novozhilov nonlinear shell theory to model the deformations. The governing equations were obtained using Hamilton's principle; it was shown that the experimental results are in good agreement with the proposed dynamic model.

The nonlinear dynamics of cylindrical shell structures have been examined lately by many researchers. Zhang et al. [135] modelled the nonlinear vibrations of thin-walled hyperelastic cylindrical shells using Donnell's nonlinear shallow shell theory. Using the

Table 1 Studies on the nonlinear dynamics of hyperelastic beams

Study	Year	Hyperelastic strain energy density model	Formulation methods/Experiments	Solution methods	Analysis
Forsat [101]	2019	Neo-Hookean, Ishihara, Mooney–Rivlin, and Yeoh models	Higher-order shear deformation theory, Hamilton's principle	Galerkin's scheme, Extended Hamiltonian method	Nonlinear free vibrations of hyperelastic beams
Mirjavadi et al. [106]	2019	Neo-Hookean, Ishihara, Mooney–Rivlin, and Yeoh models	Euler–Bernoulli beam theory, Hamilton's principle	Galerkin's scheme, Extended Hamiltonian method	Nonlinear free vibrations of hyperelastic tubes
Wang et al. [109, 112]	2018, 2019	Neo-Hookean model	The leading order model for finite deformation, Hamilton's principle	Multi-scale perturbation techniques Galerkin's method	Nonlinear vibrations of axially moving hyperelastic beams
Khaniki et al. [113]	2020	Arruda–Boyce (Eight-Chain), neo-Hookean, Gent, and Yeoh models	Experimental analysis, Euler–Bernoulli beam theory, Hamilton's principle, von Kármán theory	Galerkin's scheme, Dynamic equilibrium technique	Nonlinear forced vibrations of axially moving hyperelastic beams
Mirparizi and Fotuhi [114]	2020	Mooney-Rivlin strain energy model	Helmholtz's free energy function	Direct iteration method	Wave propagation in thermo-hyperelastic beams
Khaniki et al. [115]	2021	Mooney-Rivlin model	Experimental analysis, Euler–Bernoulli beam theory, Hamilton's principle, von Kármán theory	Galerkin's scheme, Dynamic equilibrium technique	Nonlinear forced vibration of porous-hyperelastic beams
Khaniki et al. [120]	2022	Mooney-Rivlin strain energy model	Euler–Bernoulli, Timoshenko, third-order, trigonometric and exponential beam theories, von Kármán theory, Hamilton's principle	Galerkin's scheme, Dynamic equilibrium technique	Nonlinear forced vibration of sandwich thick hyperelastic beams
Wang and Zhu [121, 122]	2021, 2021	Neo-Hookean model	Euler–Bernoulli beam theory,1 Hamilton's principle	Harmonic balance method, Galerkin's scheme	Nonlinear vibrations of axially loaded hyperelastic beams
Alibakhshi et al. [127]	2021	Gent model	Euler–Bernoulli beam theory, Hamilton's principle, modified couple stress theory, von Kármán theory	Multiple Scales Method	Nonlinear vibrations of small-scale hyperelastic beams

Lagrange equation together with the Mooney–Rivlin strain energy density model, the equations of motion were obtained. It was shown that radius-to-thickness ratio has a significant effect in changing the radial vibration behaviour. Figure 23 shows the Poincare section and bifurcation diagram of the hyperelastic cylindrical shell for different excitation forces. Xu et al. [136, 137] examined the nonlinear dynamics of

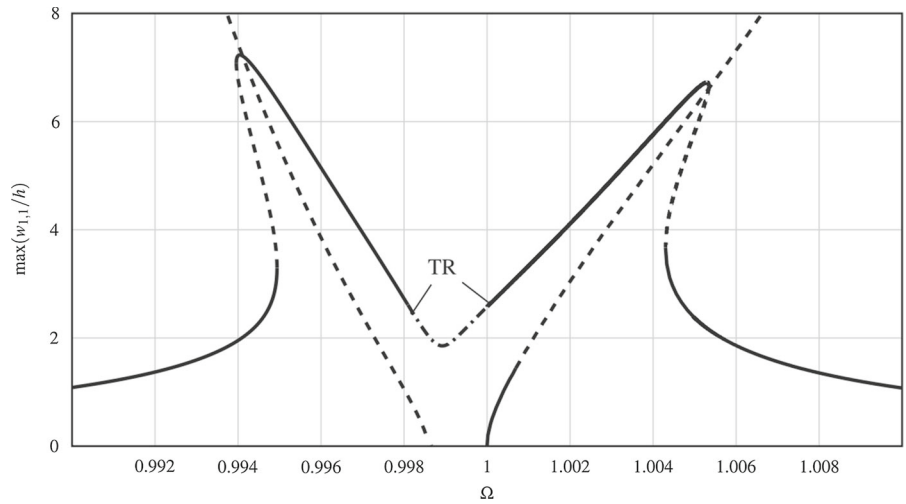

Fig. 22 Amplitude–frequency response and backbone curves of the first mode of vibration of a rectangular hyperelastic plate with two peaks associated with the 2:1 in-plane resonance [133]. (Permission obtained from ELSEVIER)

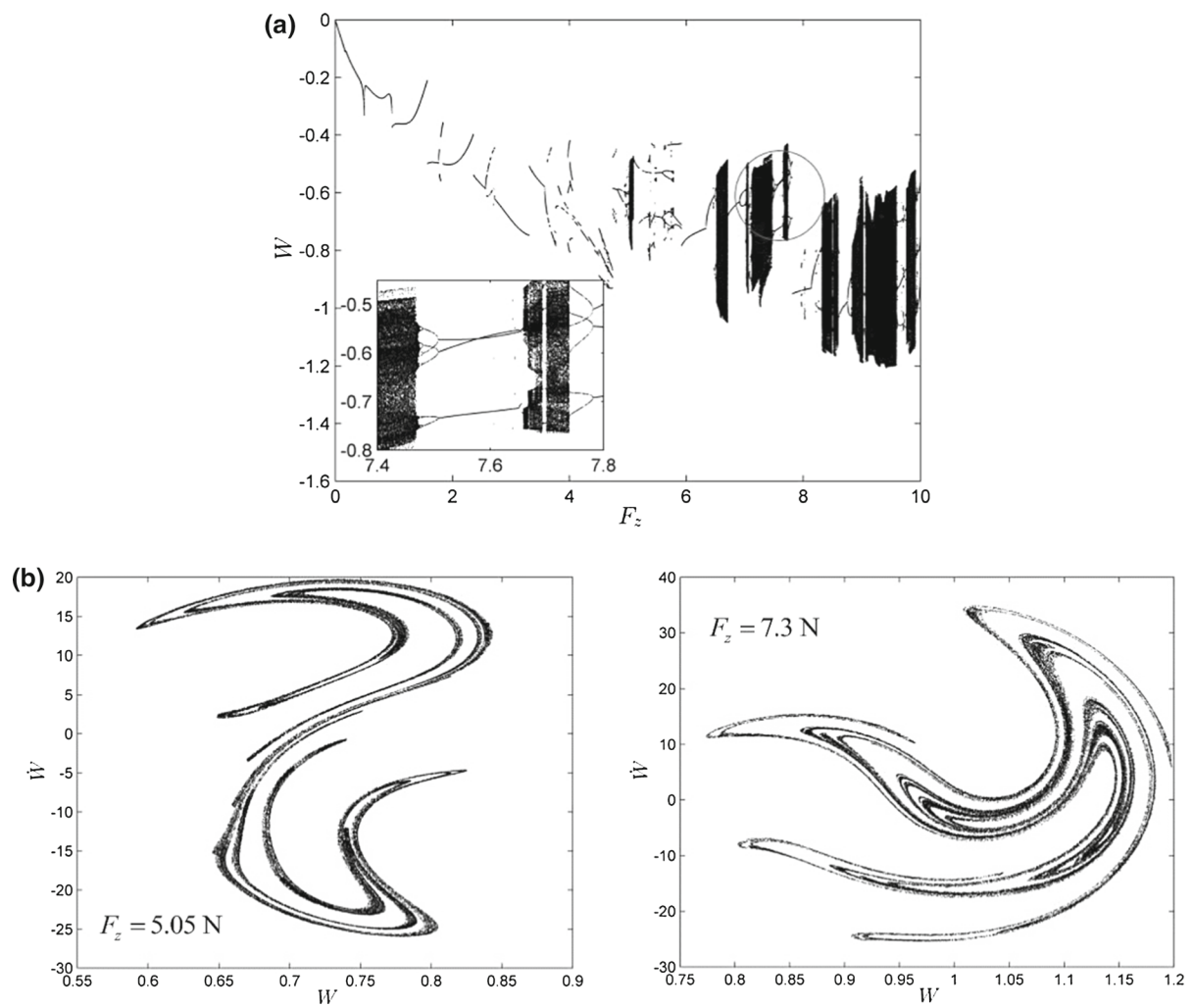

Fig. 23 **a** Bifurcation diagram and **b** Poincaré sections of a thin-walled Mooney–Rivlin cylindrical shell for different excitation forces [135]. (Permission obtained from Springer Nature)

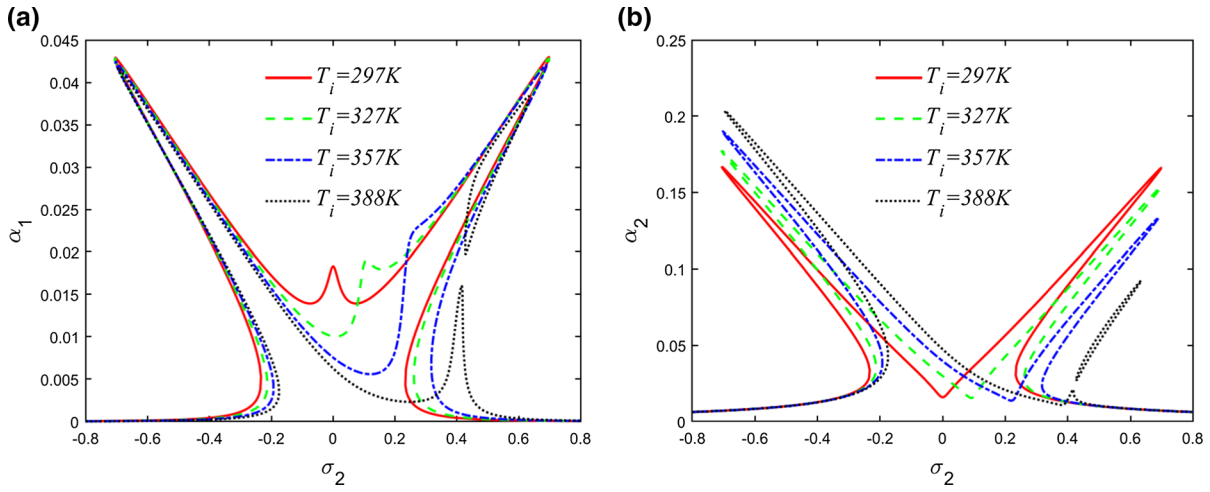

Fig. 24 The nonlinear response of the cylindrical shell with different temperature loads for the (**a**) axisymmetric and (**b**) asymmetric modes [136]. (Permission obtained from WSPC)

thin and thick hyperelastic cylindrical shells subjected to a time-dependant thermal load. It was shown that the single-mode model of such structures gives inaccurate results and the diameter-to-length ratio has a significant influence in the internal resonance phenomena. Figure 24 shows the nonlinear response of the cylindrical shell with different temperature loads for the axisymmetric and asymmetric modes. Breslavsky et al. [44, 138] investigated the free and forced nonlinear responses of circular cylindrical hyperelastic shells and square hyperelastic plates in the framework of large deformations. Hyperelasticity was modelled using the neo-Hookean model in conjunction with the Fung model, while the shell was assumed to be made of arterial bio-tissues. It was shown that the single-mode response is weak; however, the resonant response considering both companion and driven modes, was found with nonlinear complicated dynamics.

In the case of analysing electrostrictive–hyperelastic structures, Tripathi and Bajaj [139, 140] studied the internal resonances due to transverse vibration when designing hyperelastic and electrostrictive–hyperelastic plates. The Mooney–Rivlin and neo-Hookean hyperelastic strain energy models were investigated, while the plate was modelled using Kirchhoff plate theory. These showed that for nearly incompressible structures, the level of nonlinearity in the strain energy model of neo-Hookean is insufficient to lead to 1:2 internal resonances. A visco-hyperelastic model was presented by Zhao et al. [141] for modelling the chaotic motion of spherical shells. Other studies on the dynamic behaviour of hyperelastic plates and shells can be found in refs [142–148], emphasising the importance of considering hyperelasticity in studying the dynamic response of such structures. Studies on the nonlinear dynamics of hyperelastic plates and shells are summarised in Table 2.

5 Nonlinear dynamics of hyperelastic membranes and balloons

Comprehending the nonlinear dynamics of hyperelastic membranes and balloons has been a challenging task for researchers in the past few years. For circular membranes, Goncalves et al. [149, 150] studied the nonlinear vibration behaviour of isotropic homogeneous circular hyperelastic membranes stretched radially. Hyperelasticity was modelled using the neo-Hookean strain energy density model, and the motion equations were derived via Hamilton's principle. Natural frequencies were obtained analytically and compared with finite element modelling. It was revealed that all the hyperelastic models, namely the Arruda–Boyce model, Ogden model, Yeoh model and Mooney–Rivlin model, present similar nonlinear frequency–amplitude responses, qualitatively. The influence of the pre-stretch ratio on the nonlinear

Table 2 Studies on the nonlinear dynamics of hyperelastic plates/shells

Study	Year	Hyperelastic strain energy density model	Formulation methods/ Experiments	Solution methods	Analysis
Breslavsky et al. [133]	2014	Neo-Hookean model	Von Kármán non-linear plate theory, Lagrange equation	Fourier expansion, Pseudo-arc-length continuation and collocation method	Nonlinear forced vibrations of hyperelastic plates
Amabili et al. [134]	2016	Mooney-Rivlin model	Experimental analysis, Novozhilov nonlinear shell theory	Finite-element coding, Analytical procedure, Meshless approach	Nonlinear free vibrations of hyperelastic thin plates
Zhang et al. [135]	2019	Mooney-Rivlin model	Donnell's nonlinear shallow shell theory, Kirchhoff–Love hypothesis, Lagrange equation	Fourth-order Runge–Kutta method	Nonlinear vibrations of cylindrical hyperelastic shells
Xu et al. [136, 137]	2020, 2021	Arruda–Boyce model	Reddy's third-order shear deformation theory, Kirchhoff–love hypothesis, Lagrange equation	Multiple-scale method, Harmonic balance method	Nonlinear thermal vibrations of cylindrical hyperelastic shells
Breslavsky et al. [138]	2016	Neo-Hookean and Fung models	Lagrange equation, nonlinear higher-order shear deformation theory	Fourier expansion, Pseudo-arc-length continuation and collocation method	Nonlinear forced vibrations of cylindrical hyperelastic shells
Breslavsky et al. [44]	2014	Neo-Hookean, Mooney–Rivlin, and Ogden models	Lagrange equation, Novozhilov nonlinear shell theory	Fourier expansion, Pseudo-arc-length continuation and collocation method	Nonlinear forced vibrations of hyperelastic thin plates
Tripathi and Bajaj [139, 140]	2016, 2014	Neo-Hookean and Mooney–Rivlin models	Thin plate Kirchhoff theory, Lagrange equation	Method of averaging FE software	Topology optimisation and internal resonance in hyperelastic plates
Zhao et al. [141]	2020	Gent model	Finite deformation theory	Perturbation theory	Nonlinear dynamics of spherical viscoelastic hyperelastic shells
Iglesias et al. [142, 143]	2018, 2015	Seven invariants orthotropic model	Theory of a generalised Cosserat membrane	Poincaré maps and Lyapunov exponents	Nonlinear vibrations of orthotropic hyperelastic cylinders
Mason, and Maluleke [144]	2007	Mooney–Rivlin model	Ermakov–Pinney equation, First Integral Theorem of Mean Value	Lie point symmetry generator	Nonlinear radial vibrations of hyperelastic shells
Xu et al. [145]	2019	Yeoh model	Experimental analysis, Spatial tridimensional higher-order plate element, Lagrange equation	Newton–Raphson iteration and Newmark numerical techniques	Nonlinear dynamics of thick hyperelastic plates
Iglesias et al. [146]	2017	Mooney–Rivlin and Ogden models	Finite differences modelling	FE software	Nonlinear oscillations of hyperelastic shells
Wang et al. [148]	2021	Mooney–Rivlin model	Hamilton's principle, Classical theory of thermo-elasticity	Analytical and numerical solutions	Nonlinear wave propagation over thermo-hyperelastic cylindrical shells

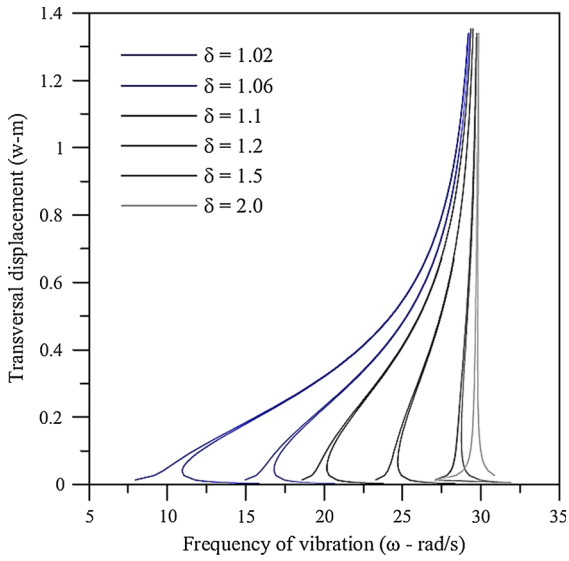

Fig. 25 Amplitude–frequency responses of hyperelastic circular membranes for different pre-stretch ratios [149]. (Permission obtained from ELSEVIER)

amplitude–frequency response of the circular hyperelastic membrane can be seen in Fig. 25.

The nonlinear breathing motion of hyperelastic spherical membranes has been examined by Soares et al. [151] using an incompressible isotropic Mooney–Rivlin strain energy density model. It was shown that the linear viscous damping term has a significant effect in changing the nonlinear resonance behaviour of the spherical membranes (Fig. 26).

Since it was shown by Mangan and Destrade [152] that the hyperelastic Gent–Gent model shows a good accuracy in modelling the nonlinear elasticity of inflated balloons, Alibakhshi and Heidari [59] used this model for studying the chaotic motion of dielectric elastomer balloons; it was shown that the chaotic motion of the dielectric elastomer balloons could be suppressed by the presence of the second invariant term in the Gent–Gent model (Fig. 27). Ilssar and Gat [153] examined the fluid–structure interaction of liquid-filled balloons using the incompressible Mooney–Rivlin strain energy density model. By verifying the model with results obtained from the finite element scheme, it was shown that the simplified presented model was capable of studying the static and

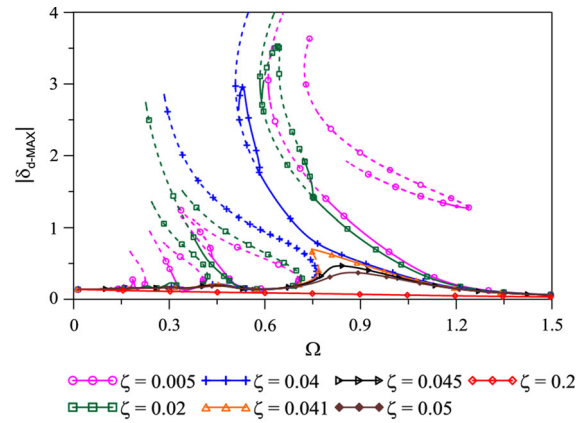

Fig. 26 The nonlinear resonance response of hyperelastic spherical membranes for different linear damping parameters [151]. (Permission obtained from Springer Nature)

dynamic behaviour of such structures. Other studies on the dynamic behaviour of hyperelastic membranes and balloons can be found in refs [19, 154–156]. Studies on the nonlinear dynamics of hyperelastic balloons and membranes are summarised in Table 3.

6 Summary and conclusions

Over the past few decades, accurately modelling the hyperelastic behaviour of polymeric structures has been a challenging task in terms of the complexity in both material and structural nonlinearities. Dozens of constitutive hyperelastic models have been presented by researchers for different materials, which some of the most practical and well-known isotropic models are presented and formulated, and the characteristics of each model are discussed. In terms of the case studies, each of these models has advantages and disadvantages in terms of accurate and inaccurate modelling for material nonlinearity and computational time cost.

Hyperelastic structures, such as rubbers and elastomers, have been analysed in different shapes and mechanical conditions. Most studies into these types of structures have been published over the past few years, since their applications are only now becoming understood. Recently, novel outcomes from rubbery

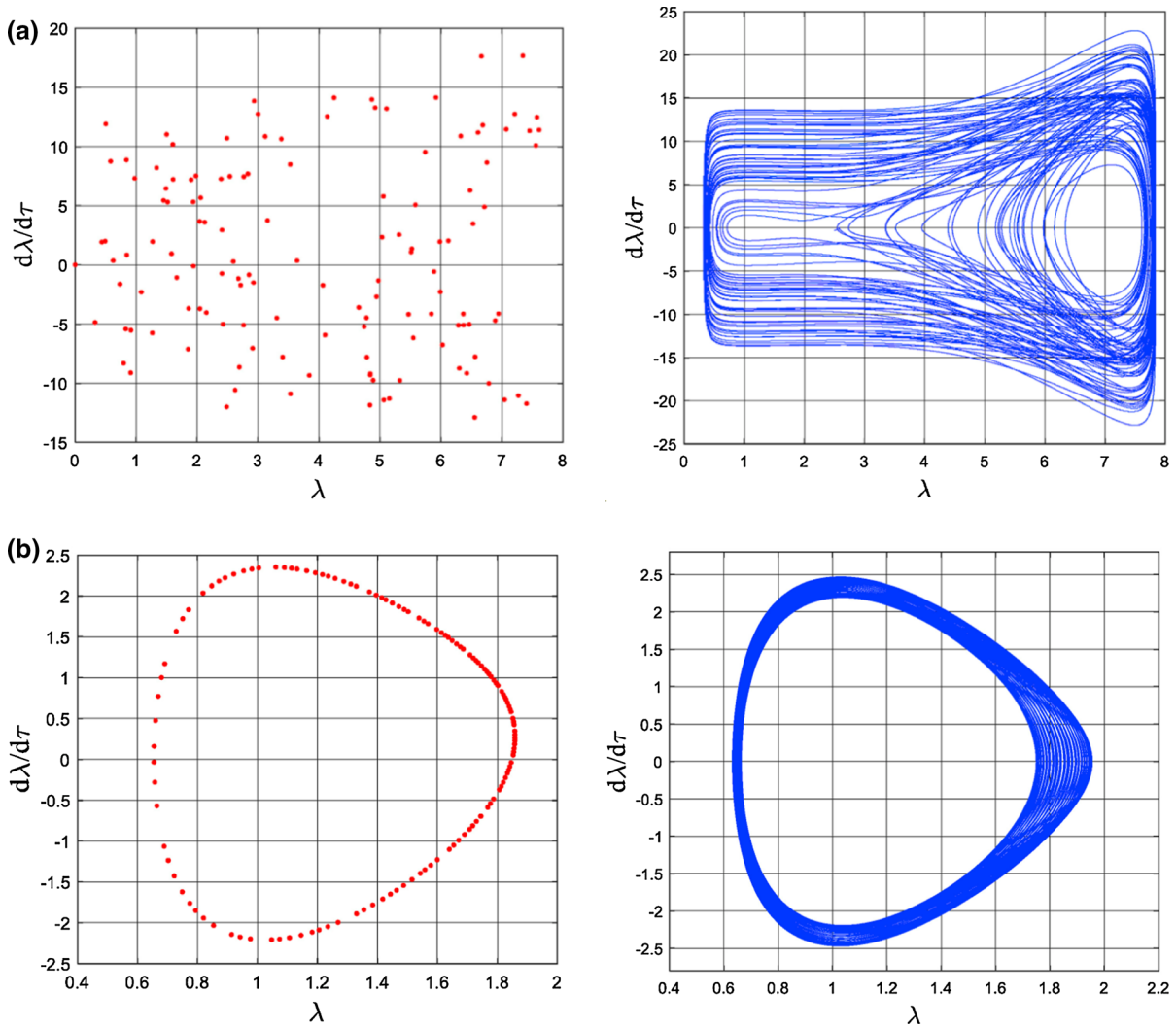

Fig. 27 Variation of the motion from **a** chaotic motion to **b** quasiperiodic vibration by increasing the second invariant parameter of the Gent–Gent model in the dielectric elastomer balloons [59]. (Permission obtained from ELSEVIER)

structures in soft robotics have moved forward such study significantly, notably in terms of achieving smooth deformations and higher the degrees of freedom. The high potential for the application of soft-based structures helped researchers to realise the importance of modelling the dynamic behaviour of hyperelasticity accurately. To demonstrate the achievements and investigations made into hyperelastic structures, a comprehensive review was presented for different structures types (beams, plates, shells, membranes and balloons) in the frameworks of nonlinear dynamics. It was shown that there has been progress in simulating the hyperelastic dynamic response using various continuum mechanic techniques in conjunction with hyperelastic strain energy density models. Since the theoretical modelling of such structures could require highly complex and long theoretical models, many studies in this field are based on simplified models ignoring the higher terms of displacement and strain. Furthermore, since soft

Table 3 Studies on the nonlinear dynamics of hyperelastic membranes/balloons

Study	Year	Hyperelastic strain energy density model	Formulation methods/ Experiments	Solution methods	Analysis
Goncalves et al. [149]	2009	Neo-Hookean, Mooney–Rivlin, Yeoh, Arruda–Boyce, and Ogden models	Lagrange function, Halmilton's principle	Galerkin method, Reduced order models, Floquet theory	Nonlinear dynamics of hyperelastic circular membranes
Soares and Goncalves [150]	2012	Neo-Hookean model	Lagrange function	Shooting method, Galerkin method	Instability and nonlinear oscillation of hyperelastic circular membranes
Soares et al. [151]	2020	Neo-Hookean and Mooney–Rivlin models	Lagrange function	Continuation techniques, Floquet theory	Nonlinear dynamics of hyperelastic spherical shells
Alibakhshi and Heidari [59]	2020	Gent-Gent model	Euler–Lagrange energy method	Time integration-based solver	Chaotic motion of hyperelastic balloons
Ilssar and Gat [153]	2020	Mooney–Rivlin model	Reduced order model	Finite-element simulations, semi-analytical model	Deflation and inflation of fluid filled hyperelastic balloons
Dong et al. [19]	2016	Yeoh model	Generic lumped parameter model, Experimental analysis	Finite element software, analytical solutions	Nonlinear dynamics of hyperelastic membrane energy harvesters
Verron et al. [154]	1999	Mooney–Rivlin model	Conservation of momentum equation	sixth-order Runge–Kutta method	Nonlinear inflation behaviour of spherical hyperelastic membranes
Li et al. [155]	2018	Gent model	Principle of virtual work, Theory of dielectric elastomers	Analytical solution	Nonlinear vibrations of dielectric hyperelastic membranes
Chaudhuri and DasGupta [156]	2014	Mooney–Rivlin model	Perturbation dynamics, Lagrange function	Iterative Ritz method	Wrinkling in inflated circular hyperelastic membranes

structures largely deform when subjected to external loads, the importance of using appropriate nonlinear large-deformation modelling is undeniable.

In summary, by analysing more than 150 research works related to this field from basic analysis to specified simulations, it can be seen that although there have been several studies on each subject of hyperelastic structure behaviour, the field is under-researched and requires further investigations to model and analyse hyperelastic structures.

Acknowledgements The HDR scholarship support through The University of Adelaide and Faculty of Engineering, Computer & Mathematical Sciences, the University of Adelaide, is acknowledged.

Funding Open Access funding enabled and organized by CAUL and its Member Institutions. The authors have not disclosed any funding.

Data availability The authors have not disclosed any funding. The datasets generated during the current study are available from the corresponding author on reasonable request.

Declarations

Conflict of interest The authors declare that there is no conflict of interest with respect to the research, authorship and/or publication of this paper.

References

1. Chen, L., et al.: Design and modeling of a soft robotic surface with hyperelastic material. Mech. Mach. Theory **130**, 109–122 (2018)
2. Case, J.C., White, E.L., Kramer, R.K.: Soft material characterization for robotic applications. Soft Rob. **2**(2), 80–87 (2015)
3. Vignali, E., et al.: Modeling biomechanical interaction between soft tissue and soft robotic instruments: importance of constitutive anisotropic hyperelastic formulations. Int. J. Rob. Res. **40**(1), 224–235 (2021)
4. Polygerinos, P., et al.: Soft robotic glove for combined assistance and at-home rehabilitation. Robot. Auton. Syst. **73**, 135–143 (2015)
5. Yap, H.K., et al.: Design and preliminary feasibility study of a soft robotic glove for hand function assistance in stroke survivors. Front. Neurosci. **11**, 547 (2017)
6. Wang, B., et al. Design and development of a glove for post-stroke hand rehabilitation. In: 2017 IEEE international conference on advanced intelligent mechatronics (AIM). 2017. IEEE
7. Proulx, C.E., et al.: Review of the effects of soft robotic gloves for activity-based rehabilitation in individuals with reduced hand function and manual dexterity following a neurological event. J Rehabil Assist Technol Eng **7**, 2055668320918130 (2020)
8. Polygerinos, P., et al.: EMG controlled soft robotic glove for assistance during activities of daily living. In 2015 IEEE international conference on rehabilitation robotics (ICORR), IEEE
9. Antol, J. and J.F. P Calhoun, *Low CostMars Surface Exploration: the Mars Tumbleweed*. Washington DC: National Aeronauticsand Space Administration. NASA/TM-2003–212411
10. Trivedi, D., Lotfi, A., Rahn, C.D.: Geometrically exact models for soft robotic manipulators. IEEE Trans. Rob. **24**(4), 773–780 (2008)
11. Kumar, V., et al.: Supporting information for microengineered materials with self-healing features for soft robotics. Authorea Preprints, (2021)
12. Liu, J., et al.: Current research, key performances and future development of search and rescue robots. Front. Mech. Eng. China **2**(4), 404–416 (2007)
13. Kumar, V., et al.: Dragonfly inspired smart soft robot. bioRxiv, (2020)
14. Wallin, T., Pikul, J., Shepherd, R.: 3D printing of soft robotic systems. Nat. Rev. Mater. **3**(6), 84 (2018)
15. Schaffner, M., et al.: 3D printing of robotic soft actuators with programmable bioinspired architectures. Nat. Commun. **9**(1), 878 (2018)
16. Yap, H.K., Ng, H.Y., Yeow, C.-H.: High-force soft printable pneumatics for soft robotic applications. Soft Rob. **3**(3), 144–158 (2016)
17. He, L., et al.: Variational modeling of plane-strain hyperelastic thin beams with thickness-stretching effect. Acta Mech. **229**(12), 4845–4861 (2018)
18. Chen, Y., Jin, L.: Snapping-back buckling of wide hyperelastic columns. Extreme Mech. Lett. **34**, 100600 (2019)
19. Dong, L., et al.: Application of mechanical stretch to tune the resonance frequency of hyperelastic membrane-based energy harvesters. Sens. Actuators, A **252**, 165–173 (2016)
20. Tang, X., et al.: A soft crawling robot driven by single twisted and coiled actuator. Sens. Actuators, A **291**, 80–86 (2019)
21. Chen, T., Lee, D., Sung, C.-K.: An experimental study on transmission efficiency of a rubber V-belt CVT. Mech. Mach. Theory **33**(4), 351–363 (1998)
22. Bertini, L., Carmignani, L., Frendo, F.: Analytical model for the power losses in rubber V-belt continuously variable transmission (CVT). Mech. Mach. Theory **78**, 289–306 (2014)
23. Kolosov, A.: The stress-strain state of the belt in the operating changes of the burdening conveyor parameters. In: Theoretical and Practical Solutions of Mineral Resources Mining, pp. 585–590. CRC Press (2015)
24. Esse, R., *Flexible packaging end-use market analysis.* Linthicum, Md.: Flexible Packaging Assn, (2002)
25. Brody, A.L., et al.: Innovative food packaging solutions. J. Food Sci. **73**(8), 107–116 (2008)
26. Siracusa, V., et al.: Biodegradable polymers for food packaging: a review. Trends Food Sci. Technol. **19**(12), 634–643 (2008)
27. Dilkes-Hoffman, L.S., et al.: Environmental impact of biodegradable food packaging when considering food waste. J. Clean. Prod. **180**, 325–334 (2018)
28. Muller, J., González-Martínez, C., Chiralt, A.: Combination of poly (lactic) acid and starch for biodegradable food packaging. Materials **10**(8), 952 (2017)
29. Kim, H.S., Nonlinear multi-scale anisotropic material and structural models for prosthetic and native aortic heart valves. (2009) Georgia Institute of Technology
30. Schendel, M.J. and C.F. Popelar: Numerical methods for design and evaluation of prosthetic heart valves, in Heart Valves. (2013), Springer. pp. 321-341
31. Dickinson, A., Steer, J., Worsley, P.: Finite element analysis of the amputated lower limb: a systematic review and recommendations. Med. Eng. Phys. **43**, 1–18 (2017)

32. Mohammadi, H., Mequanint, K.: Prosthetic aortic heart valves: modeling and design. Med. Eng. Phys. **33**(2), 131–147 (2011)
33. Zolfagharian, A., Kaynak, A., Kouzani, A.: Closed-loop 4D-printed soft robots. Mater. Des. **188**, 108411 (2019)
34. Ijaz, S., et al.: Magnetically actuated miniature walking soft robot based on chained magnetic microparticles-embedded elastomer. Sens. Actuators, A **301**, 111707 (2020)
35. Bonet, J., Wood, R.D.: Nonlinear continuum mechanics for finite element analysis. Cambridge University Press, Cambridge (1997)
36. Holzapfel, G.A.: Nonlinear solid mechanics: a continuum approach for engineering science. Meccanica **37**(4–5), 489–490 (2002)
37. Bower, A.F.: Applied mechanics of solids. CRC Press, London (2009)
38. Steck, D., et al.: Mechanical responses of Ecoflex silicone rubber: compressible and incompressible behaviors. J. Appl. Polym. Sci. **136**(5), 47025 (2019)
39. Moerman, K.M., Fereidoonnezhad, B., McGarry, J.P.: Novel hyperelastic models for large volumetric deformations. Int. J. Solids Struct. **193**, 474–491 (2020)
40. Pelliciari, M., Tarantino, A.M.: Equilibrium paths for von Mises trusses in finite elasticity. J. Elast. **138**(2), 145–168 (2020)
41. Bertram, A.: Elasticity and plasticity of large deformations. (2012) Springer
42. Capurro, M. and F. Barberis: Evaluating the mechanical properties of biomaterials. In: Biomaterials for Bone Regeneration. (2014), Elsevier. pp. 270–323
43. Brown, C., et al.: Assessment of common hyperelastic constitutive equations for describing normal and osteoarthritic articular cartilage. Proc. Inst. Mech. Eng. [H] **223**(6), 643–652 (2009)
44. Breslavsky, I.D., Amabili, M., Legrand, M.: Nonlinear vibrations of thin hyperelastic plates. J. Sound Vib. **333**(19), 4668–4681 (2014)
45. Mooney, M.: A theory of large elastic deformation. J. Appl. Phys. **11**(9), 582–592 (1940)
46. Falope, F.O., et al.: Snap-through and Eulerian buckling of the bi-stable von Mises truss in nonlinear elasticity: a theoretical, numerical and experimental investigation. Int. J. Non-Linear Mech. **134**, 103739 (2021)
47. Rivlin, R.: Large elastic deformations of isotropic materials IV. Further developments of the general theory. Philos. Trans. R. Soc. Lond. Ser. A Math. Phys. Sci. **241**(835), 379–397 (1948)
48. Rivlin, R.: Large elastic deformations of isotropic materials VI. Further results in the theory of torsion, shear and flexure. Philos. Trans. R. Soc. Lond. Ser. A Math. Phys. Sci. **242**(845), 173–195 (1949)
49. Biderman, V., Calculation of rubber parts. Rascheti na prochnost, 1958. **40**.
50. Klosner, J.M. and A. Segal: Mechanical characterization of a natural rubber (1969)
51. James, A., Green, A., Simpson, G.: Strain energy functions of rubber. I. Characterization of gum vulcanizates. J. Appl. Polym. Sci. **19**(7), 2033–2058 (1975)
52. Marckmann, G., Verron, E.: Comparison of hyperelastic models for rubber-like materials. Rubber Chem. Technol. **79**(5), 835–858 (2006)
53. Ogden, R.: Large deformation isotropic elasticity—On the correlation of theory and experiment for incompressible rubberlike solids. Rubber Chem. Technol. **46**(2), 398–416 (1973)
54. Ogden, R.W.: Large deformation isotropic elasticity–on the correlation of theory and experiment for incompressible rubberlike solids. Proc. R. Soc. Londn. A Math. Phys. Sci. **326**(1567), 565–584 (1972)
55. Arruda, E.M., Boyce, M.C.: A three-dimensional constitutive model for the large stretch behavior of rubber elastic materials. J. Mech. Phys. Solids **41**(2), 389–412 (1993)
56. Liu, Y., A.E. Kerdok, and R.D. Howe. A nonlinear finite element model of soft tissue indentation. In: international symposium on medical simulation (2004) Springer
57. Gent, A.: A new constitutive relation for rubber. Rubber Chem. Technol. **69**(1), 59–61 (1996)
58. Gent, A.: Elastic instabilities of inflated rubber shells. Rubber Chem. Technol. **72**(2), 263–268 (1999)
59. Alibakhshi, A., Heidari, H.: Nonlinear dynamics of dielectric elastomer balloons based on the Gent-Gent hyperelastic model. Eur. J. Mech.-A/Solids **82**, 103986 (2020)
60. Horgan, C.O.: The remarkable Gent constitutive model for hyperelastic materials. Int. J. Non-Linear Mech. **68**, 9–16 (2015)
61. Destrade, M., Annaidh, A.N., Coman, C.D.: Bending instabilities of soft biological tissues. Int. J. Solids Struct. **46**(25–26), 4322–4330 (2009)
62. Goriely, A., Destrade, M., Amar, M.B.: Instabilities in elastomers and in soft tissues. Q. J. Mech. Appl. Math. **59**(4), 615–630 (2006)
63. Horgan, C., Saccomandi, G.: A description of arterial wall mechanics using limiting chain extensibility constitutive models. Biomech. Model. Mechanobiol. **1**(4), 251–266 (2003)
64. Roland, C.M., Viscoelastic behavior of rubbery materials. 2011: OUP Oxford
65. Bischoff, J.E., Arruda, E.M., Grosh, K.: A new constitutive model for the compressibility of elastomers at finite deformations. Rubber Chem. Technol. **74**(4), 541–559 (2001)
66. Mac Donald, B.J.: Practical stress analysis with finite elements. Glasnevin Publishing, Dublin (2007)
67. Horgan, C.O., Saccomandi, G.: Constitutive models for compressible nonlinearly elastic materials with limiting chain extensibility. J. Elast. **77**(2), 123–138 (2004)
68. Beda, T.: Modeling hyperelastic behavior of rubber: a novel invariant-based and a review of constitutive models. J. Polym. Sci., Part B: Polym. Phys. **45**(13), 1713–1732 (2007)
69. Blatz, P.J., Ko, W.L.: Application of finite elastic theory to the deformation of rubbery materials. Trans. Soc. Rheol. **6**(1), 223–252 (1962)
70. Murnaghan, F.D.: Finite deformations of an elastic solid. Am. J. Math. **59**(2), 235–260 (1937)
71. Ciarlet, P.G.: Mathematical Elasticity: Volume I: three-dimensional elasticity. (1988): North-Holland
72. Valanis, K., Landel, R.F.: The strain-energy function of a hyperelastic material in terms of the extension ratios. J. Appl. Phys. **38**(7), 2997–3002 (1967)

73. Hill, R.: Aspects of invariance in solid mechanics, advances in applied mechanics, pp. 1–75. Elsevier, London (1979)
74. Attard, M.M.: Finite strain—isotropic hyperelasticity. Int. J. Solids Struct. **40**(17), 4353–4378 (2003)
75. Bischoff, J., Arruda, E., Grosh, K.: A microstructurally based orthotropic hyperelastic constitutive law. J. Appl. Mech. **69**(5), 570–579 (2002)
76. Itskov, M.: A generalized orthotropic hyperelastic material model with application to incompressible shells. Int. J. Numer. Meth. Eng. **50**(8), 1777–1799 (2001)
77. Latorre, M., Montáns, F.J.: Material-symmetries congruency in transversely isotropic and orthotropic hyperelastic materials. Eur. J. Mech.-A/Solids **53**, 99–106 (2015)
78. Motevalli, M., et al.: Geometrically nonlinear simulation of textile membrane structures based on orthotropic hyperelastic energy functions. Compos. Struct. **223**, 110908 (2019)
79. Bonet, J., Burton, A.: A simple orthotropic, transversely isotropic hyperelastic constitutive equation for large strain computations. Comput. Methods Appl. Mech. Eng. **162**(1–4), 151–164 (1998)
80. Itskov, M., Aksel, N.: A class of orthotropic and transversely isotropic hyperelastic constitutive models based on a polyconvex strain energy function. Int. J. Solids Struct. **41**(14), 3833–3848 (2004)
81. Diani, J., et al.: Directional model for isotropic and anisotropic hyperelastic rubber-like materials. Mech. Mater. **36**(4), 313–321 (2004)
82. Sun, S. and W. Chen: An anisotropic hyperelastic constitutive model with bending stiffness interaction for cord-rubber composites: comparison of simulation results with experimental data. Math. Probl. Eng., 2020. **2020**
83. Gültekin, O., Dal, H., Holzapfel, G.A.: On the quasi-incompressible finite element analysis of anisotropic hyperelastic materials. Comput. Mech. **63**(3), 443–453 (2019)
84. Chaimoon, K., Chindaprasirt, P.: An anisotropic hyperelastic model with an application to soft tissues. Eur. J. Mech.-A/Solids **78**, 103845 (2019)
85. Cai, R., et al.: A new hyperelastic model for anisotropic hyperelastic materials with one fiber family. Int. J. Solids Struct. **84**, 1–16 (2016)
86. Nolan, D.R., et al.: A robust anisotropic hyperelastic formulation for the modelling of soft tissue. J. Mech. Behav. Biomed. Mater. **39**, 48–60 (2014)
87. Chen, Z.-W., Joli, P., Feng, Z.-Q.: Anisotropic hyperelastic behavior of soft biological tissues. Comput. Methods Biomech. Biomed. Engin. **18**(13), 1436–1444 (2015)
88. Guerin, H.L., Elliott, D.M.: Quantifying the contributions of structure to annulus fibrosus mechanical function using a nonlinear, anisotropic, hyperelastic model. J. Orthop. Res. **25**(4), 508–516 (2007)
89. Peng, X., et al.: A simple anisotropic hyperelastic constitutive model for textile fabrics with application to forming simulation. Compos. B Eng. **52**, 275–281 (2013)
90. Fernández, M., et al.: Anisotropic hyperelastic constitutive models for finite deformations combining material theory and data-driven approaches with application to cubic lattice metamaterials. Comput. Mech. **67**(2), 653–677 (2021)
91. De Marco, C., et al.: Indirect 3D and 4D printing of soft robotic microstructures. Adv. Mater. Technol. **4**(9), 1900332 (2019)
92. Yang, Y., et al.: Hybrid jamming for bioinspired soft robotic fingers. Soft Rob. **7**(3), 292–308 (2020)
93. Lee, J.-H., Chung, Y.S., Rodrigue, H.: Long shape memory alloy tendon-based soft robotic actuators and implementation as a soft gripper. Sci. Rep. **9**(1), 1–12 (2019)
94. Ji, X., et al.: An autonomous untethered fast soft robotic insect driven by low-voltage dielectric elastomer actuators. Sci. Robot. **4**(37), 6451 (2019)
95. Irschik, H., Gerstmayr, J.: A hyperelastic Reissner-type model for non-linear shear deformable beams. Proc. Mathmod. **9**, 1–7 (2009)
96. Irschik, H., Gerstmayr, J.: A continuum-mechanics interpretation of Reissner's non-linear shear-deformable beam theory. Math. Comput. Model. Dyn. Syst. **17**(1), 19–29 (2011)
97. Jiang, F., Yu, W.: Nonlinear variational asymptotic sectional analysis of hyperelastic beams. AIAA J. **54**(2), 679–690 (2015)
98. Lanzoni, L., Tarantino, A.M.: Finite anticlastic bending of hyperelastic solids and beams. J. Elast. **131**(2), 137–170 (2018)
99. Wang, R., et al.: Radially and axially symmetric motions of a class of transversely isotropic compressible hyperelastic cylindrical tubes. Nonlinear Dyn. **90**(4), 2481–2494 (2017)
100. Ogden, R.W.: Non-linear elastic deformations. Courier Corporation, United States (1997)
101. Forsat, M.: Investigating nonlinear vibrations of higher-order hyper-elastic beams using the Hamiltonian method. Acta Mech. **231**, 125–138 (2019)
102. Lotfan, S., et al.: Nonlinear resonances of axially functionally graded beams rotating with varying speed including Coriolis effects. Nonlinear Dyn. **107**(1), 533–558 (2022)
103. Tian, Y., Daeichin, M., Towfighian, S.: Dynamic behavior of T-beam resonator with repulsive actuation. Nonlinear Dyn. **107**(1), 15–31 (2022)
104. Ghayesh, M.H.: Dynamical analysis of multilayered cantilevers. Commun. Nonlinear Sci. Numer. Simul. **71**, 244–253 (2019)
105. Ghayesh, M.H.: Asymmetric viscoelastic nonlinear vibrations of imperfect AFG beams. Appl. Acoust. **154**, 121–128 (2019)
106. Mirjavadi, S.S., Forsat, M., Badnava, S.: Nonlinear modeling and dynamic analysis of bioengineering hyper-elastic tubes based on different material models. Biomech. Model. Mechanobiol. **19**, 971–983 (2019)
107. Pham, P.-T., Hong, K.-S.: Dynamic models of axially moving systems: a review. Nonlinear Dyn. **100**(1), 315–349 (2020)
108. Chen, L.-Q., Tang, Y.-Q., Lim, C.W.: Dynamic stability in parametric resonance of axially accelerating viscoelastic Timoshenko beams. J. Sound Vib. **329**(5), 547–565 (2010)
109. Wang, Y., Ding, H., Chen, L.-Q.: Vibration of axially moving hyperelastic beam with finite deformation. Appl. Math. Model. **71**, 269–285 (2019)
110. Zhu, X., Wang, Y., Lou, Z.: A study of the critical strain of hyperelastic materials: a new kinematic frame and the

leading order term. Mech. Res. Commun. **78**, 20–24 (2016)
111. Chen, W., Wang, L., Dai, H.: Nonlinear free vibration of hyperelastic beams based on neo-Hookean model. Int. J. Struct. Stab. Dyn. **20**(01), 2050015 (2020)
112. Wang, Y., Ding, H., Chen, L.-Q.: Nonlinear vibration of axially accelerating hyperelastic beams. Int. J. Non-Linear Mech. **99**, 302–310 (2018)
113. Khaniki, H.B., et al.: Experimental characteristics and coupled nonlinear forced vibrations of axially travelling hyperelastic beams. Thin-Wall. Struct. **170**, 108526 (2022)
114. Mirparizi, M., Fotuhi, A.: Nonlinear coupled thermo-hyperelasticity analysis of thermal and mechanical wave propagation in a finite domain. Physica A **537**, 122755 (2020)
115. Khaniki, H.B., et al.: Large amplitude vibrations of imperfect porous-hyperelastic beams via a modified strain energy. J. Sound Vib. **513**, 116416 (2021)
116. Ügdüler, S., et al.: Towards closed-loop recycling of multilayer and coloured PET plastic waste by alkaline hydrolysis. Green Chem. **22**(16), 5376–5394 (2020)
117. Schulze, M., et al.: Evaluation of a panel of spermatological methods for assessing reprotoxic compounds in multilayer semen plastic bags. Sci. Rep. **10**(1), 1–11 (2020)
118. Ramos, M.J.G., Lozano, A., Fernández-Alba, A.R.: High-resolution mass spectrometry with data independent acquisition for the comprehensive non-targeted analysis of migrating chemicals coming from multilayer plastic packaging materials used for fruit purée and juice. Talanta **191**, 180–192 (2019)
119. Walker, T.W., et al.: Recycling of multilayer plastic packaging materials by solvent-targeted recovery and precipitation. Sci. Adv. **6**(47), 7599 (2020)
120. Khaniki, H.B., et al.: Nonlinear continuum mechanics of thick hyperelastic sandwich beams using various shear deformable beam theories. Cont. Mech. Thermodyn. **34**, 781–827 (2022)
121. Wang, Y., Zhu, W.: Nonlinear transverse vibration of a hyperelastic beam under harmonic axial loading in the subcritical buckling regime. Appl. Math. Model. **94**, 597–618 (2021)
122. Wang, Y., Zhu, W.: Nonlinear transverse vibration of a hyperelastic beam under harmonically varying axial loading. J. Comput. Nonlinear Dyn. **16**(3), 031006 (2021)
123. Faghihi, S., et al.: Graphene oxide/poly (acrylic acid)/gelatin nanocomposite hydrogel: experimental and numerical validation of hyperelastic model. Mater. Sci. Eng., C **38**, 299–305 (2014)
124. Pelliciari, M., Tarantino, A.M.: Equilibrium and stability of anisotropic hyperelastic graphene membranes. J. Elast. **144**(2), 169–195 (2021)
125. Pelliciari, M., Tarantino, A.M.: A nonlinear molecular mechanics model for graphene subjected to large in-plane deformations. Int. J. Eng. Sci. **167**, 103527 (2021)
126. Höller, R., Libisch, F., Hellmich, C.: A membrane theory for circular graphene sheets, based on a hyperelastic material model for large deformations. Mech. Adv. Mater. Struct. **29**(5), 651–661 (2022)
127. Alibakhshi, A., et al.: Nonlinear free and forced vibrations of a hyperelastic micro/nanobeam considering strain stiffening effect. Nanomaterials **11**(11), 3066 (2021)
128. Yang, F., et al.: Couple stress based strain gradient theory for elasticity. Int. J. Solids Struct. **39**(10), 2731–2743 (2002)
129. Ma, H., Gao, X.-L., Reddy, J.: A microstructure-dependent Timoshenko beam model based on a modified couple stress theory. J. Mech. Phys. Solids **56**(12), 3379–3391 (2008)
130. Park, S., Gao, X.: Bernoulli-Euler beam model based on a modified couple stress theory. J. Micromech. Microeng. **16**(11), 2355 (2006)
131. Ghayesh, M.H.: Nonlinear dynamics of multilayered microplates. J. Comput. Nonlinear Dyn. **13**(2), 021006 (2018)
132. Ghayesh, M.H.: Mechanics of tapered AFG shear-deformable microbeams. Microsyst. Technol. **24**(4), 1743–1754 (2018)
133. Breslavsky, I.D., Amabili, M., Legrand, M.: Physically and geometrically non-linear vibrations of thin rectangular plates. Int. J. Non-Linear Mech. **58**, 30–40 (2014)
134. Amabili, M., et al.: Experimental and numerical study on vibrations and static deflection of a thin hyperelastic plate. J. Sound Vib. **385**, 81–92 (2016)
135. Zhang, J., et al.: Nonlinear vibration analyses of cylindrical shells composed of hyperelastic materials. Acta Mech. Solida Sin. **32**(4), 463–482 (2019)
136. Xu, J., et al.: Nonlinear vibrations of thermo-hyperelastic moderately thick cylindrical shells with 2: 1 internal resonance. Int. J. Struct. Stab. Dyn. **20**(05), 2050067 (2020)
137. Xu, J., et al.,: Internal resonance of hyperelastic thin-walled cylindrical shells under harmonic axial excitation and time-varying temperature field (2021)
138. Breslavsky, I.D., Amabili, M., Legrand, M.: Static and dynamic behavior of circular cylindrical shell made of hyperelastic arterial material. J. Appl. Mech. **83**(5), 051002 (2016)
139. Tripathi, A., Bajaj, A.K.: Topology optimization and internal resonances in transverse vibrations of hyperelastic plates. Int. J. Solids Struct. **81**, 311–328 (2016)
140. Tripathi, A., Bajaj, A.K.: Design for 1: 2 internal resonances in in-plane vibrations of plates with hyperelastic materials. J. Vib. Acoust. **136**(6), 061005 (2014)
141. Zhao, Z., et al.: Nonlinear dynamics of loaded visco-hyperelastic spherical shells. Nonlinear Dyn. **101**(2), 911–933 (2020)
142. Aranda-Iglesias, D., Rodríguez-Martínez, J., Rubin, M.: Nonlinear axisymmetric vibrations of a hyperelastic orthotropic cylinder. Int. J. Non-Linear Mech. **99**, 131–143 (2018)
143. Aranda-Iglesias, D., Vadillo, G., Rodríguez-Martínez, J.: Constitutive sensitivity of the oscillatory behaviour of hyperelastic cylindrical shells. J. Sound Vib. **358**, 199–216 (2015)
144. Mason, D., Maluleke, G.: Non-linear radial oscillations of a transversely isotropic hyperelastic incompressible tube. J. Math. Anal. Appl. **333**(1), 365–380 (2007)
145. Xu, Q., Liu, J and Qu, L.: A higher-order plate element formulation for dynamic analysis of hyperelastic silicone plate. J Mech pp 1–14
146. Aranda-Iglesias, D., Vadillo, G., Rodríguez-Martínez, J.: Oscillatory behaviour of compressible hyperelastic shells

subjected to dynamic inflation: a numerical study. Acta Mech. **228**(6), 2187–2205 (2017)
147. Amabili, M., Breslavsky, I., Reddy, J.: Nonlinear higher-order shell theory for incompressible biological hyperelastic materials. Comput. Methods Appl. Mech. Eng. **346**, 841–861 (2019)
148. Wang, R., et al.: Nonlinear singular traveling waves in a slightly compressible thermo-hyperelastic cylindrical shell. Nonlinear Dyn. **107**(2), 1495–1509 (2022)
149. Gonçalves, P.B., Soares, R.M., Pamplona, D.: Nonlinear vibrations of a radially stretched circular hyperelastic membrane. J. Sound Vib. **327**(1–2), 231–248 (2009)
150. Soares, R.M., Gonçalves, P.B.: Nonlinear vibrations and instabilities of a stretched hyperelastic annular membrane. Int. J. Solids Struct. **49**(3–4), 514–526 (2012)
151. Soares, R.M., et al.: Nonlinear breathing motions and instabilities of a pressure-loaded spherical hyperelastic membrane. Nonlinear Dyn. **99**(1), 351–372 (2020)
152. Mangan, R., Destrade, M.: Gent models for the inflation of spherical balloons. Int. J. Non-Linear Mech. **68**, 52–58 (2015)
153. Ilssar, D., Gat, A.D.: On the inflation and deflation dynamics of liquid-filled, hyperelastic balloons. J. Fluids Struct. **94**, 102936 (2020)
154. Verron, E., et al.: Dynamic inflation of hyperelastic spherical membranes. J. Rheol. **43**(5), 1083–1097 (1999)
155. Li, Y., et al.: Nonlinear dynamic analysis and active control of visco-hyperelastic dielectric elastomer membrane. Int. J. Solids Struct. **152**, 28–38 (2018)
156. Chaudhuri, A., DasGupta, A.: On the static and dynamic analysis of inflated hyperelastic circular membranes. J. Mech. Phys. Solids **64**, 302–315 (2014)